Article
MESSENGER
Vol. 3, 35–51, 2014
www.aspbs.com/messenger

Design, Synthesis, and Chemical and Biological Properties of Cyclic ADP-4-Thioribose as a Stable Equivalent of Cyclic ADP-Ribose

Takayoshi Tsuzuki[1], Satoshi Takano[1], Natsumi Sakaguchi[1], Takashi Kudoh[1], Takashi Murayama[3], Takashi Sakurai[3], Minako Hashii[4], Haruhiro Higashida[4], Karin Weber[5], Andreas H. Guse[5], Tomoshi Kameda[6], Takatsugu Hirokawa[6], Yasuhiro Kumaki[7], Mitsuhiro Arisawa[1], Barry V. L. Potter[8], and Satoshi Shuto[1, 2, *]

[1] *Faculty of Pharmaceutical Sciences,* [2] *Center for Research and Education on Drug Discovery, Hokkaido University, Kita-12, Nishi-6, Kita-ku, Sapporo 060-0812, Japan*
[3] *Department of Pharmacology, Juntendo University School of Medicine, 2-1-1 Hongo, Bunkyo-ku, Tokyo 113-8421, Japan*
[4] *Department of Biophysical Genetics, Takaramachi, Kanazawa University Graduate School of Medicine, Kanazawa 920-8640, Japan*
[5] *The Calcium Signalling Group, University Medical Center Hamburg-Eppendorf, Center of Experimental Medicine, Department of Biochemistry and Signal Transduction, Martinistr. 52, 20246 Hamburg, Germany*
[6] *Computational Biology Research Center, National Institute of Advanced Industrial Science and Technology, Aomi, Koutou-ku, Tokyo 135-0064, Japan*
[7] *Faculty of Sciences, Hokkaido University, Kita-11, Nishi-8, Kita-ku, Sapporo 060-0812, Japan*
[8] *Wolfson Laboratory of Medicinal Chemistry, Department of Pharmacy and Pharmacology, University of Bath, Claverton Down, Bath BA2 7AY, UK*

Here we describe the successful synthesis of cyclic ADP-4-thioribose (cADPtR, 3), designed as a stable mimic of cyclic ADP-ribose (cADPR, 1), a Ca^{2+}-mobilizing second messenger, in which the key N1-β-thioribosyladenosine structure was stereoselectively constructed by condensation between the imidazole nucleoside derivative 8 and the 4-thioribosylamine 7 via equilibrium in 7 between the α-anomer (7α) and the β-anomer (7β) during the reaction course. cADPtR is, unlike cADPR, chemically and biologically stable, while it effectively mobilizes intracellular Ca^{2+} like cADPR in various biological systems, such as sea urchin homogenate, NG108-15 neuronal cells, and Jurkat T-lymphocytes. Thus, cADPtR is a stable equivalent of cADPR, which can be useful as a biological tool for investigating cADPR-mediated Ca^{2+}-mobilizing pathways.

Keywords: Cyclic ADP-Ribose, cADPR, Second Messenger, Ca^{2+}-Release.

INTRODUCTION

Cyclic ADP-ribose (cADPR, **1**, Fig. 1), a metabolite of NAD^+ (nicotinamide adenine dinucleotide), was originally isolated from sea urchin by Lee and co-workers (Clapper et al., 1987). cADPR mobilizes intracellular Ca^{2+} in various mammalian cells, such as, pancreatic β-cells, smooth muscle, cardiac muscle, T-lymphocytes, and cerebellar neurons, and therefore, cADPR is now recognized as a general mediator of intracellular Ca^{2+} signaling (Galione, 1993; Lee, 1997; Galione et al., 1998; Guse, 1999; Higashida et al., 2001; Lee, 2002; Guse, 2004; Zhang and Li, 2006; Jin et al., 2007; Venturi et al., 2010; Lee, 2012).

Analogs of cADPR have been extensively designed and synthesized, since they are potentially useful for investigating the mechanism of cADPR-mediated Ca^{2+} release (Walseth and Lee, 1993; Lee et al., 1993; Zhang and Sih, 1995; Ashamu et al., 1995; Wagner et al., 2003, 2005; Moreau et al., 2006, 2012; Galeone et al., 2002; Huang et al., 2002; Gu et al., 2004; Xu et al., 2006; Swarbrick and Potter, 2012; Yu et al., 2012; Shuto et al., 1998; Fukuoka et al., 2000; Shuto et al., 2001; Guse et al., 2002; Shuto et al., 2003; Kudoh et al., 2005; Hashii et al., 2005; Kudoh et al., 2008; Zhang et al., 1999; Shuto and Matsuda, 2004; Guse, 2004; Potter and Walseth, 2004). cADPR analogs are also expected to be lead structures for

*Author to whom correspondence should be addressed.
E-mail: shu@pharm.hokudai.ac.jp

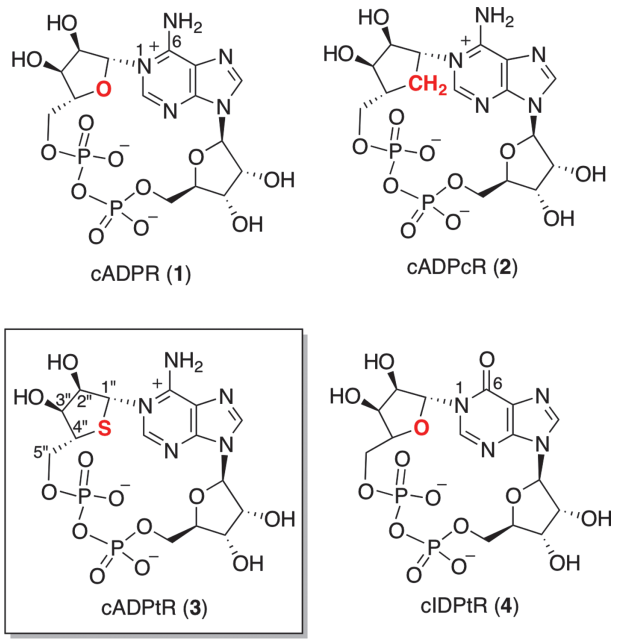

Figure 1. cADPR (1), cADPcR (2), cADPtR (3) and cIDPR (4).

the development of potential drug candidates, due to the important physiological roles of cADPR (Galione, 1993; Lee, 1997; Galione 1998; Guse, 1999; Higashida et al., 2001; Lee, 2002; Guse, 2004; Zhang, 2006; Jin et al., 2007; Venturi et al., 2010; Lee, 2012). cADPR analogs have been synthesized predominantly by enzymatic and chemo-enzymatic methods using ADP-ribosyl cyclase-catalyzed cyclization under mild conditions (Walseth and Lee, 1993; Lee et al. 1993; Zhang and Sih, 1995; Ashamu et al., 1995; Wagner et al., 2003, 2005; Moreau et al., 2006, 2012). The analogs obtained by these methods, however, are limited due to the substrate-specificity of the ADP-ribosyl cyclase (Zhang et al., 1999; Shuto and Matsuda, 2004; Guse, 2004; Potter and Walseth, 2004).

In recent years, methods for the chemical synthesis of cADPR analogs have been studied to develop useful cADPR analogs (Galeone et al., 2002; Huang et al., 2002; Gu et al., 2004; Xu et al., 2006; Swarbrick et al., 2012; Yu et al., 2012; Shuto et al., 1998; Fukuoka et al., 2000; Shuto et al., 2001; Guse et al., 2002; Shuto et al., 2003; Kudoh et al., 2005; Hashii et al., 2005; Kudoh et al., 2008; Zhang et al., 1999; Shuto et al., 2004; Gusu et al., 2004; Potter et al., 2004). Construction of the characteristic pyrophosphate-containing 18-membered ring structure is the key to the synthesis of cADPR and its analogs, and we have developed an efficient method for forming the ring using *S*-phenyl phosphorothioate-type substrates, which can be effectively activated by Ag^+ or I_2 (Fukuoka et al., 2000; Shuto et al., 2001).

cADPR is readily hydrolyzed at the unstable N1-ribosyl linkage to produce ADP-ribose (ADPR), even in neutral aqueous solution (Lee and Aarhus, 1993). This is due to the fact that cADPR is in a zwitterionic form positively charged around the N1-C6-N^6 moiety ($pK_a = 8.3$), making the molecule unstable, where the charged adenine moiety attached to the anomeric carbon of the N1-linked ribose is able to be an efficient leaving group. Under physiological conditions, cADPR is also hydrolyzed at the same N1-ribosyl linkage by cADPR hydrolase to give the inactive ADPR (Lee and Aarhus, 1993).

We previously designed and synthesized cyclic ADP-carbocyclic-ribose (cADPcR, **2**) as a stable mimic of cADPR, in which the oxygen atom in the N1-ribose ring of cADPR is replaced by a methylene group. cADPcR is both chemically and biologically stable, and effectively mobilizes intracellular Ca^{2+} in sea urchin eggs (Shuto et al., 2001). Although cADPcR is more potent than cADPR in neuronal cells (Hashii et al., 2005), it is almost inactive in T cells, whereas natural cADPR effectively mobilizes Ca^2 in both neuronal cells and T cells (Guse et al., 2002; Kudoh et al., 2005).

Although intensive studies of the signaling pathway that uses cADPR are still needed because of its biological importance, the biological as well as chemical instability of cADPR limits further studies of its physiological role. Therefore, stable analogs of cADPR exhibiting Ca^{2+}-mobilizing activity in various cells including T cells are required. Thus, we newly designed and synthesized a 4-thioribose-containing analog of cADPR, i.e., cyclic ADP-4-thioribose (cADPtR, **3**), in which the N1-ribose of cADPR is replaced by a 4-thioribose. Evaluations in several biological systems revealed that cADPtR is a stable equivalent of cADPR, which mobilizes intracellular Ca^{2+} not only in sea urchin eggs and neuronal cells, but also in T cells. Here we report the detailed results of these studies on cADPtR.

RESULTS AND DISCUSSION

Design of cADPtR

cADPR is in an equilibrium between the N^6-protonated amino-form and the N^6-deprotonated imino-form, as shown in Figure 2 (Lee et al., 1989; Kim et al., 1993; Lee et al., 1994; Gu and Sih, 1994; Wada et al., 2005; Wada and Pope, 2001; Graham et al., 2004). One difference between cADPR and cADPcR is their pK_a values for protonation at the N^6-position. The pK_a of cADPcR (8.9) (Guse et al., 2002) is somewhat higher than that of cADPR (8.3) (Kim et al., 1994), which might affect its interaction with target proteins. Under physiological conditions, cADPR is in a mixture of the protonated amino form and the deprotonated imino form, where most of cADPcR should be present in the amino-form due to its relatively higher pK_a. If cADPR binds to the target protein in T cells in the imino-form, activity of cADPcR would be decreased. In recent years, cADPR analogs with a hypoxanthine base instead of an adenine base, such as cyclic IDP-ribose (cIDPR, **4**, Fig. 1), were synthesized,

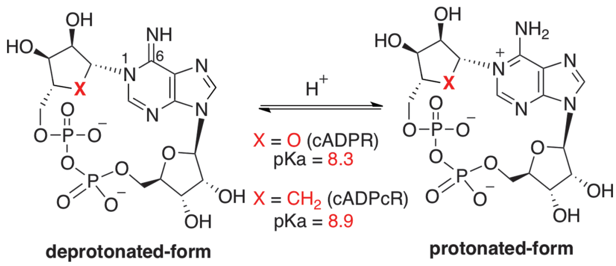

Figure 2. **Equilibrium between the N^6-protonated amino-form and the N^6-deprotonated imino-form in cADPR and cADPcR.**

and these hypoxanthine-type analogs also mobilized Ca^{2+} in T cells, while they were almost inactive in other biological sytems (Moreau et al., 2006; Huang et al., 2002; Gu et al., 2004; Xu et al., 2006). These findings support the idea of an active imino-form of cADPR in T cells, because the $C6{=}O^6$ moiety might work as a bioisostere of the plane $C6{=}N^6$ moiety of the imino-form of cADPR, due to their analogous unsaturated π-electronic structural features.

Another difference between cADPR and cADPcR might be their three-dimensional structures. In nucleosides, conformation around the glycoside linkage is one of the determinants of their biological activities, and they generally prefer a conformation that avoids steric repulsion between the nucleobase and sugar moieties (Saenger, 1983). Therefore, in cADPR and its analogs, the most stable conformation can be the one with minimal steric repulsion between the adenine moiety and both of the N1- and N9-ribose moieties. It should be noted that, in cADPcR, the hydrogens on the tetrahedral sp^3-C6″-, particularly the H6″-β, which is absent in cADPR, are rather sterically repulsive to the adenine H2 (Fig. 3). Accordingly, the stable conformation of cADPcR would differ from that of cADPR due to the steric effects (Kudoh et al., 2008).

Taking these considerations into account, we newly designed cADPtR, a 4-thioribose analog of cADPR. 4″-Thionucleosides are recognized as useful bioisosteres of the natural nucleosides, which are extensively used in studies of medicinal chemistry and chemicalbiology (Reist et al., 1964; Bobek and Whistler, 1970; Dyson et al., 1991; Bellon et al., 1993; Yoshimura et al., 1997; Naka et al., 2000; Takahashi et al., 2009). The 4-thioribose in 4″-thionucleosides does not only effectively mimics the ribose

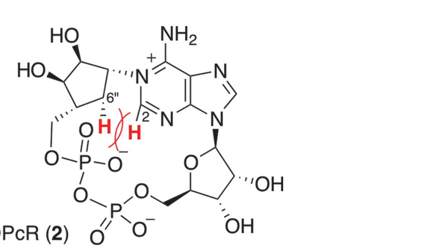

cADPcR (**2**)

Figure 3. **Possible steric repulsion between the H2 and the H6″β.**

of nucleosides, but also the N-4-thioriobyl linkage is more stable than the corresponding N-ribosyl linkage against both chemical and enzymatic hydrolysis (Elzagheid et al., 1999; Toyohara et al., 2003). In addition, the pK_a value of cADPtR is expected to be similar to that of cADPR due to the electron-withdrawing property of sulfur atom. This type of pK_a adjustment of biologically active compounds by replacing a methylene with a sulfur has been reported previously (Ganellin and Owen, 1977). Furthermore, the conformation of cADPtR, particularly spatial positioning of the N1-thioribose and adenine moieties, would be similar to that of cADPR, because both sulfur and oxygen have a similar sp^3 configuration bearing two non-bonding electron pairs. Thus, we expected that cADPtR might be a stable cADPR equivalent that is active in various cells including T cells.

Synthetic Plan

The retrosynthetic scheme for the target cADPtR (**3**) is shown in Figure 4. For the synthesis of cADPtR, construction of the 18-membered pyrophosphate structure is an important step. The structure was likely to be constructed using the intramolecular condensation reaction with an *S*-phenyl phosphorothioate-type substrate that we developed (Fukuoka et al., 2000; Shuto et al., 2001), which has been effectively used in the synthesis of a variety of cADPR analogs (Galeone et al., 2002; Huang et al., 2002; Gu et al., 2004; Xu et al., 2006; Swarbrick et al., 2012; Yu et al., 2012). Thus, treatment of the *S*-phenyl phosphorothioate-type substrates **5** having the N1-4-thioribosyladenosine structure with $AgNO_3$/MS3A as a promoter (Fukuoka et al., 2000; Shuto et al., 2001) would form the desired cyclization product, and subsequent deprotection would furnish the target cADPtR. The *S*-phenyl phosphorothioate-type substrates **5** would be obtained from the N1-β-thioribosyl adenosine derivative **6**β, which we planned to construct by condensation between the 4-thioribosylamine **7** and a known imidazole nucleoside derivative **8** (Hutchinson et al., 1997) readily prepared from inosine. The 4-thioribosylamine **7** was expected to be prepared from the 1-deoxy-4-thioribose derivative **9**, obtained by a known method (Jeong et al., 2006).

In this synthetic plan, we first had to achieve stereoselective construction of the N1-β-thioribosyladenosine structure. Although no 4-thioribse derivatives having an anomeric amino function such as **7** have been reported to date, 4-thioribosylamine **7** is likely to be present as an anomeric mixture, due to the electron-donating property of the hemiaminal ether nitrogen attaching at the anomeric position. We speculated that if the 4-thioribosylamine derivative **7** is indeed in equilibrium between the α-anomer (**7**α) and the β-anomer (**7**β), stereoselective construction of the N1-β-thioribosyladenosine structure might be

MESSENGER MESSENGER MESSENGER MESSENGER MESSENGER MESSENGER

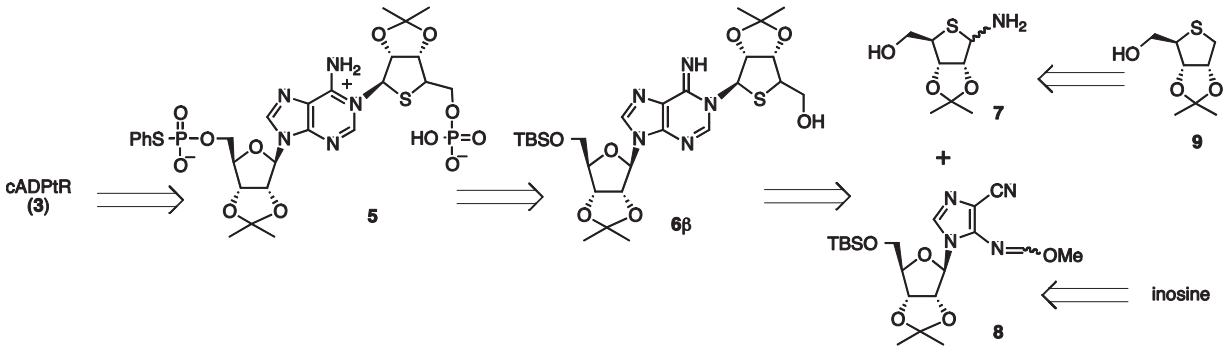

Figure 4. **Retrosynthetic analysis of the target cADPtR (3).**

achieved. In the 4-thioribosylamine **7**, the α-face would be rather sterically more hindered than the β-face due to its rigid 5,5-*cis* ring system. Thus, as shown in Figure 5, in the condensation reaction, the β-anomer **7**β might preferentially react with the imidazole nucleoside **8**, while the α-anomer **7**α might not react due to the steric hindrance by the adjacent isopropylidene moiety. Thus, we expected that, in the reaction course, the relatively less reactive α-anomer would not undergo the condensation, but rather would be effectively converted into the more reactive β-anomer via the equilibrium to result in accumulation of the desired β-condensation product **6**β.

Synthesis

The 4-thioribosylamine **7** was prepared from the known 1-deoxy-4-thioribose derivative **9** (Jeong et al., 2006), as shown in Scheme 1. While several procedures for synthesizing 4-thioribose derivatives have been reported (Reist et al., 1964; Bobek and Whistler, 1970; Dyson et al., 1991; Bellon et al., 1993; Yoshimura et al., 1997; Naka et al., 2000; Takahashi et al., 2009), we selected the procedure recently developed by Jeong and co-workers (Jeong et al., 2006), which is effective for large scale preparation of the 4-thio-1-deoxyribose derivative **9** having the desired 2,3-*O*-isopropylidene protecting group. Oxidation of **9** with *m*-CPBA and subsequent heating of the resulting sulfoxide product in Ac_2O to initiate the Pummerer rearrangement afforded the 1-acetoxy product **11** as an anomeric mixture ($\alpha/\beta = 1{:}5$). When the anomeric mixture **11** was treated with $TMSN_3$ and $SnCl_4$ in CH_2Cl_2, the β-azide **12** was obtained stereoselectively in high yield, probably due to the steric demand of the reaction intermediate. Reduction of the azido group of **12** by catalytic hydrogenation, followed by removal of the *O*-acetyl group by heating it in MeOH gave the 4-thioribosylamine **7**, which appeared to be an anomeric mixture ($\alpha/\beta = 1{:}2$) as we expected.

We next investigated the key condensation between the 4-thioribosylanine **7** ($\alpha/\beta = 1{:}2$) and the imidazole nucleoside **8** under various conditions. Under basic reaction conditions, i.e., K_2CO_3/MeOH which was previously used to construct the N1-carbocyclic-ribosyladenine structures (Shuto et al., 2001), the desired β-condensation product **6b** was actually obtained stereoselectively in 50% yield. Under the conditions, however, the N^6-(4-thioribosy) product **13** via a Dimroth rearrangement was also obtained in 28% yield. As a result, we found that when **7** was treated with **8** (2.1 eq) in MeOH at room temperature without any bases, the β-product **6b** was obtained in 61% yield concomitant with 5% of the α-product **6a**, where the 4-thioribosylamine **7** was recovered in 17% yield (Scheme 2). Thus, the desired β-product **6b** was successfully obtained in 73% conversion yield from the

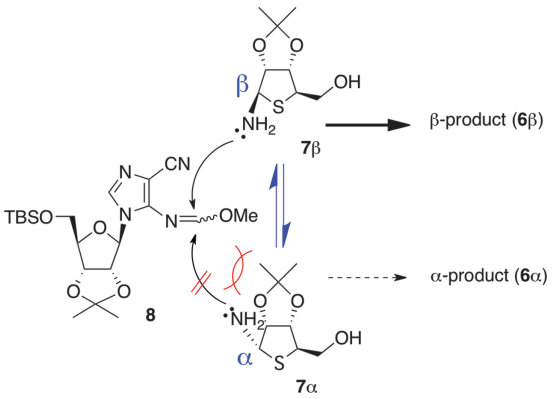

Figure 5. **Hypothesis for the stereoselective formation of the desired β-product 7β via the α/β equilibrium.**

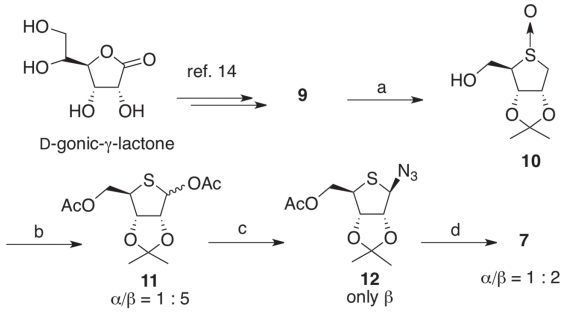

a) 1) *m*CPBA, CH_2Cl_2, –78 °C, 91%; b) Ac_2O, 100 °C, 64%; c) $TMSN_3$, $SnCl_4$, CH_2Cl_2, 0 °C, 86%; d) 1) H_2, Pd-C, MeOH, 2) MeOH, reflux, quant.

Scheme 1. Synthesis of 4-thioribosylamine **7**.

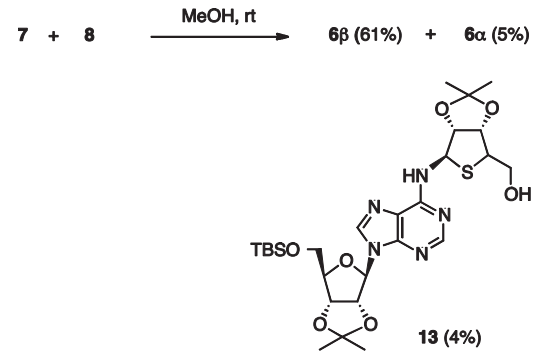

Scheme 2. Stereoselective synthesis of N1-β-thioribosyladenosine derivative **6β**.

4-thioribosylamine ($\alpha/\beta = 1{:}2$) via the α/β-equilibrium, as we hypothesized. In the reaction conditions, the N^6-thioribosyl product **13** (4%) was also obtained.

The N1-substituted structures of **6a** and **6b** was confirmed based on their HMBC spectra, in which correlation between the H2 of the adenine and the C1″ of the 4-thioribose moiety was observed. The α- and β-stereochemistries of **6a** and **6b** were confirmed by NOE data (see Fig. 11).

Conversion of the N1-β-thioribosyl product **6b** into the *S*-phenyl phosphorothioate-type substrate **5** was next investigated (Scheme 3). The 5″-hydroxy group of **6b** was protected with a dimethoxytrityl (DMTr) group, and then the 5″-*O*-TBS group of the product **14** was removed with TBAF to give **15**. Treatment of **15** with an *S*,*S*″-diphenylphosphorodithioate (PSS)/2,4,6-triisopropylbenzenesulfonyl chloride (TPSCl)/pyridine system (Sekine et al., 1985; Sekine and Hata, 1993), followed by removal of the 5‴″-*O*-DMTr group of the product **16** with aqueous AcOH gave the 5″-bis-*S*-(phenyl)phosphorothioate **17**.

We next examined phosphorylation of the 5″-hydroxyl of **17**. However, treatment of **17** under the usual conditions of Yoshikawa's phosphorylation procedure with $POCl_3/(EtO)_3PO$ (Yoshikawa et al., 1969), which was effective in the previous synthesis of cADPcR and its analogs, gave none of the desired phosphorylation product **18**.

Difficulties in the phosphorylation of the 4-thioribose moiety could be assumed to occur, at least partially, because phosphorylation of the 5″-primary hydroxyl of 4′-thioribnucleoside derivatives is rather difficult compared to the cases with usual ribonucleosides (Hancox and Walker, 1996; Alexandova et al., 1996). Walker and coworkers reported that phosphorylation of 4″-thiothymidine by Yoshikawa's procedure did not give the desired corresponding 5″-*O*-phosphate product. They suggested that elimination of the dichlorophosphate moiety would occur in an intermediate **A** due to effective neighboring group participation by the nucleophilic ring sulfur to result in reproducing the starting material 4″-thiothymidine, via a thionium intermediate **B** and its subsequent hydrolysis, as shown in Scheme 4(a) (Hancox and Walker, 1996).

We thought that a zwitterionic phosphorylating reagent **19** (Scheme 4(b)), reported by Asseline and Thuong (Asseline and Thuong et al., 1988), might be effective for the phosphorylation of **17**, because in the phosphorylation

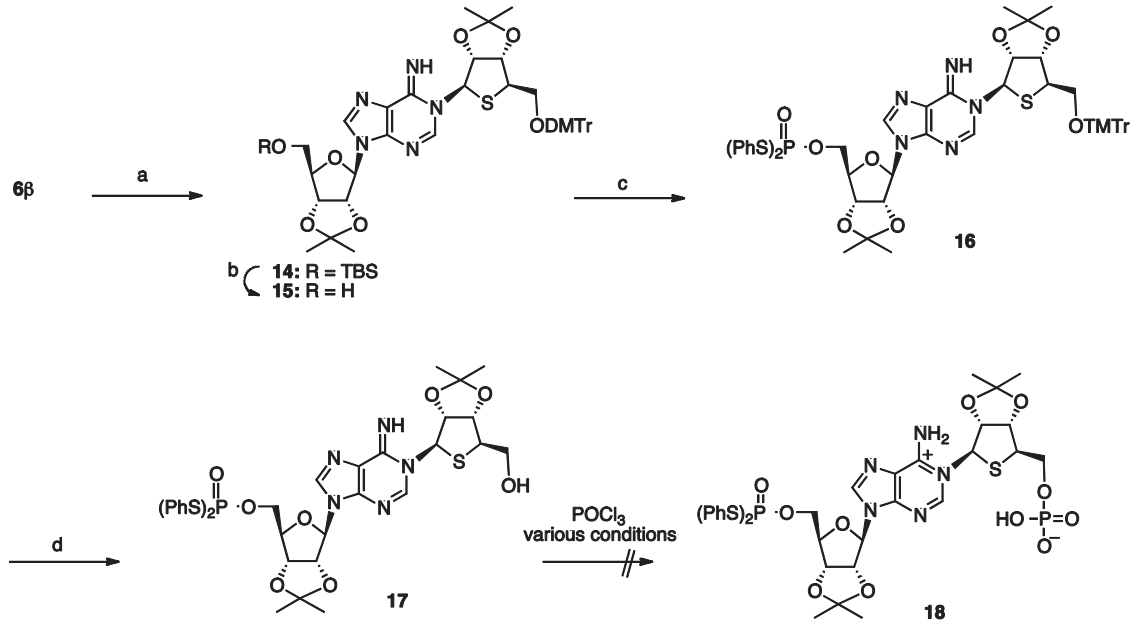

Reagents and conditions: a) DMTrCl, pyridine, rt, 81%; b) TBAF, THF, AcOH, rt, quant; c) PSS, TPSCl, pyridine, –15 °C, 72%; d) aq. AcOH, 90%.

Scheme 3. Investigation for synthesizing 5′-bis-S-(phenyl)phosphorothioate **17**.

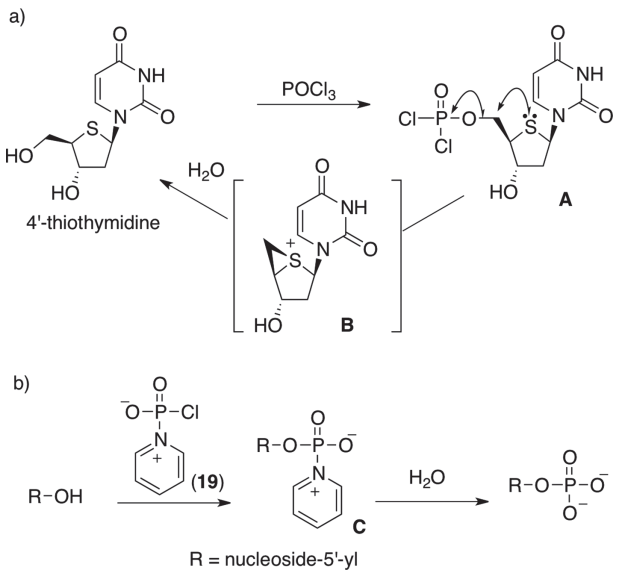

Scheme 4. Hydrolysis of 5′-dichlorophosphate **B** via intermediate **A** (a) and zwitterionic phosphorylating reagent **19** (b).

intermediate **C**, the leaving ability of the phosphate moiety would be decreased due to the negatively charged oxygen. Thus, when **17** was treated with **19** in pyridine at −30 °C and then the reaction was quenched with triethylammonium acetate (TEAA) buffer, a compound likely to be the desired phosphorylated **18** was detected as a main peak by HPLC analysis. The product, without purification, was further treated with H_3PO_2 and Et_3N in pyridine to remove the phenylthio group (Hata et al., 1987) affording the phosphorylation product **5** after purification by ion-exchange chromatography (Scheme 5).

With the *S*-phenyl phosphorothioate **5** in hand, we next investigated the intramolecular cyclization reaction. When a solution of **5** in pyridine was slowly added to a mixture of a large excess of $AgNO_3$ and Et_3N in the presence of MS3A in pyridine at room temperature (Fukuoka et al., 2000; Shuto et al., 2001), the desired cyclization product **19** was obtained in 76% yield. Finally, removal of the isopropylidene groups of **19** with aqueous HCO_2H produced the target cADPtR (**3**) in 49% yield (Scheme 5).

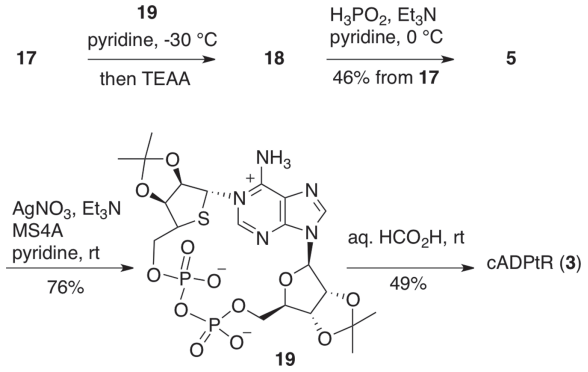

Scheme 5. Synthesis of cADPtR (3).

Stability of cADPtR

cADPtR (**3**) appeared to be rather chemically stable, since the final acidic removal of the isopropylidene groups of **20** was successful to produce cADPtR, as described above (Scheme 5).

The biological stability of cADPtR was investigated with a rat brain microsomal extract that contains cADPR degradation enzymes (Lee and Aarhus, 1993). We first treated cADPR with the extract at 37 °C to result in its rapid degradation. As expected, under the same conditions, cADPtR was almost completely resistant to degradation in the extract. After 120 min treatment, approximately 90% of cADPR disappeared, whereas most of cADPtR remained intact, indicating that cADPtR is stable under physiological conditions (see Fig. 12).

pK_a Value of cADPtR

The pK_a value of cADPtR (**3**) was determined using a previously reported method (Kim et al., 1993). This method is based on the pH-dependent UV spectral change between 285 nm and 300 nm area of cADPR or its analogs, due to the protonation and proton-dissociation at the N^6 position of the adenine ring. As a result, the pK_a of cADPtR was determined to be 8.0, which was similar to that of cADPR ($pK_a = 8.3$) (Kim et al., 1993) and about 1 unit lower than that of cADPcR ($pK_a = 8.9$) (Guse et al., 2002).

Ca^{2+}-Mobilizing Activity in Sea Urchin Egg Homogenate

We tested the Ca^{2+}-mobilizing ability of cADPtR (**3**) as well as cADPR (**1**) and cADPcR (**2**) by fluorometrically monitoring Ca^{2+} with *H. pulcherrimus* sea urchin egg homogenate (Fig. 6) (Shiwa et al., 2002). cADPR released Ca^{2+} from the homogenate in a concentration-dependent manner with an EC_{50} value of 214 nM, and cADPcR showed more potent activity ($EC_{50} = 54$ nM) than cADPR, where the maximal Ca^{2+}-mobilizing activity of cADPcR was almost equal to that of cADPR. These results are consistent with previous reports that cADPcR potently activates Ca^{2+} release in sea urchin eggs of *A. crassispina* or *L. pictus* (Shuto etal., 2001; Kudoh et al., 2008). As shown in Figure 6, cADPtR exhibited highly potent Ca^{2+}-mobilizing ability ($EC_{50} = 36$ nM), which was about 7-fold more potent than the natural second messenger cADPR and even more potent than cADPcR.

Ca^{2+}-Mobilizing Activity in Neuronal Cells

The effect of cADPtR (**3**) on cytosolic Ca^{2+} mobilization in NG108-15 neuronal cells was studied in permeabilized conditions using digitonin as the detergent (Higashida et al., 1990; Amina et al., 2010). We first verified that extracellular application of digitonin itself did

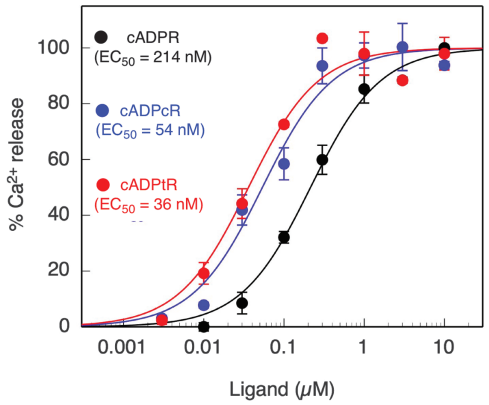

Figure 6. Concentration-dependent Ca^{2+}-mobilizing activity of cADPR, cADPcR, and cADPtR in sea urchin egg homogenate. The Ca^{2+}-mobilizing activity of each compound is expressed as the percent change in ratio of fura-2 fluorescence (F340/F380) relative to that of 10 μM cADPR. Data are mean ± SEM of 3 to 6 experiments.

not cause an increase in $[Ca^{2+}]_i$ in the conditions in which the plasma membrane was permeabilized with 250 nM of digitonin for nearly 5 min (Figs. 7(b) and (c)). We also confirmed that application of 100 mM cADPR (**1**), used as a positive control, caused a gradual and sustained Ca^{2+} release in the digitonin-permeabilized conditions, which allowed nucleotides to enter into the cytoplasm (Fig. 8(c)). When cADPR was applied extracellularly to intact NG108-15 cells, no increase in $[Ca^{2+}]_i$ was detected (data not shown). Figure 7(a) shows a representative field of cells with $[Ca^{2+}]_i$ changes induced by the application of cADPtR with the plasma cell membrane was permeabilized with 250 nM digitonin for 5 min. Figure 8(c) shows the mean time-course of $[Ca^{2+}]_i$ changes induced by cADPtR. Application of 100 μM cADPtR induced persistent increases in $[Ca^{2+}]_i$: the mean $[Ca^{2+}]_i$ level measured 4 min after application of cADPtR was 116 ± 2.3% of the resting (pre-permeabilization) level (mean ± SEM; $n = 6$). The amplitude evoked by cADPtR was equivalent to or significantly greater than that induced by cADPR: the mean $[Ca^{2+}]_i$ level measured 4 min after application of cADPR was 107 ± 2.8% of the resting level ($n = 10$). A similar Ca^{2+}-mobilizing pattern was observed in cADPcR-applied cells: the mean $[Ca^{2+}]_i$ level measured 4 min after application of cADPcR was 115 ± 3.1% of the resting level ($n = 10$).

These results in NG108-15 neuronal cells indicate that cADPtR has potent Ca^{2+}-mobilizing activity, similar to cADPcR. Both cADPtR and cADPcR have increased efficacy as compared with cADPR, which may be due to their increased metabolic stability.

Ca^{2+}-Mobilizing Activity in *T* Cells

The Ca^{2+}-mobilizing effect of cADPtR (**3**) was evaluated using saponin-permeabilized Jurkat *T* cells as reported previously (Guse et al., 1993; Guse et al., 2007; Schwarzmann et al., 2002). Both cADPtR and cADPR (**1**) evoked rapid Ca^{2+} release upon addition to the permeabilized cell suspension indicating similar mechanisms of Ca^{2+} release (Fig. 8(a)). Though cADPR was somewhat more potent at 100 mM, cADPR and cADPtR had very similar concentration-response curves (Fig. 8(b)) indicating that cADPtR binds to the cADPR receptor protein with similar affinity. Our previous work revealed that replacing the northern ribose of cADPR with the carbocyclic moiety (cADPcR) shifted its Ca^{2+} mobilizing activity to much higher concentrations (Guse et al., 2002). In contrast, the new analog cADPtR was almost as active as cADPR. A difference of cADPcR and analog cADPtR are their pK_a values, amounting to 8.9 and 8.0, respectively. Taking the pK_a value of cADPR and the indistinguishable biological activity between cIDPR (**4**) and cADPR (Moreau et al., 2006; Huang et al., 2002; Gu et al., 2004; Xu et al., 2006) in *T* cells into account, the relatively high biological activity of cADPtR might be in favour of the imino form of cADPR being the active form of the natural second messenger in *T* cells.

Conformational Analysis

The three-dimensional structures of biologically active compounds in aqueous solution is very important from the viewpoint of the bioactive conformation. Our study shows that cADPR (**1**), cADPcR (**2**), and cADPtR (**3**) have different activities in sea urchin eggs, neuronal cells and *T* cells, respectively. To investigate the biological difference based on their conformations, structures of them were constructed by molecular dynamics calculations with a simulated annealing method based on the NOE constraints of the intramolecular proton pairs measured in D_2O (for details, see Fig. 13). The structures obtained by the calculations based on their observed NOE in the NOESY spectra are shown in Figure 9.

To analyze the structural differences in more detail, these structures were superimposed as shown in Figure 10(a), which shows that the cADPtR structure (red) resembles that of natural cADPR (blue). The cADPcR structure (green), however, is not similar to those of the other two compounds, in which the relative special arrangement of the N1-thioribose ring and the adenine ring is clearly different from those of the other two compounds, as we expected. Thus, the distances between the 4″S between the adenine H2 of cADPtR (3.6 Å) is significantly longer than the corresponding distances of cADPR (2.3 Å) and cADPtR (2.5 Å), probably due to the steric repulsion between the H6″β with the adenine H2 in cADPcR.

To confirm the validity of the obtained structures, we used the cADPR structure solved by X-ray crystallographic analysis (2j, Lee et al., 1994). Thus, the X-ray

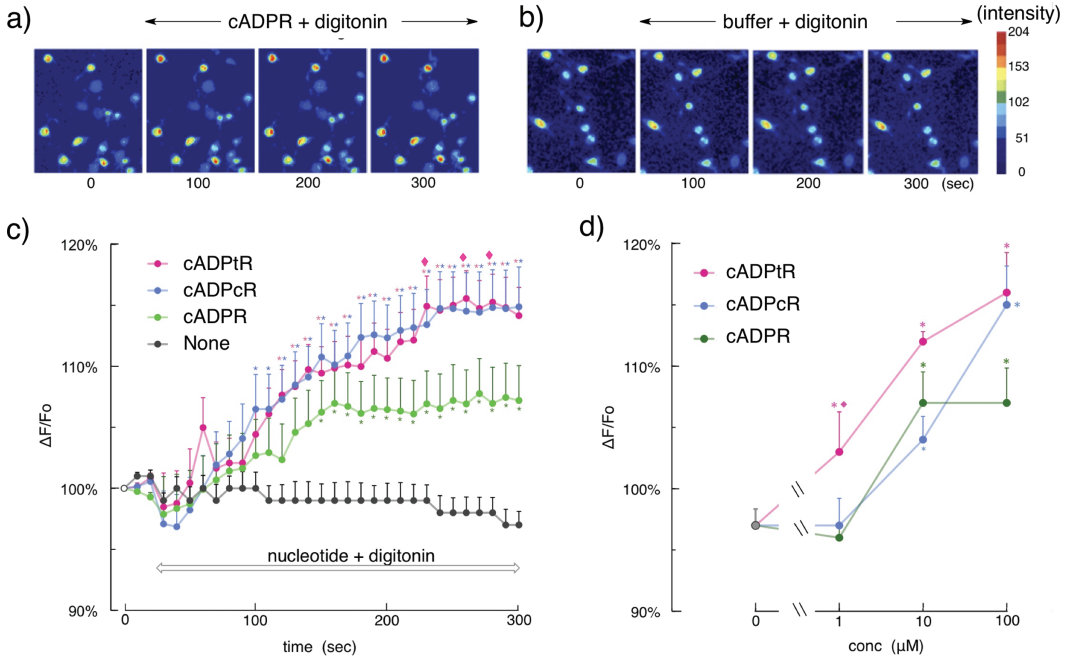

Figure 7. **Effects of cADPtR on $[Ca^{2+}]_i$ increases in permeabilized NG108-15 cells. (a), (b)** Cells were permeabilized by the addition of 250 nM digitonin to the bath solution. cADPtR (final concentration, 100 μM) **(a)** or an equal amount of buffer **(b)** was added together with digitonin as indicated by the arrows. Representative fields are displayed for each condition. Changes in $[Ca^{2+}]_i$ are shown as pseudocolor images, and colors reflecting fluorescence intensities are indicated to the right together with arbitrary units. **(c)** Time-course of $[Ca^{2+}]_i$ changes in Oregon Green-loaded NG 108–15 cells. At about 25 s after the beginning of each trace, cell membranes were permeabilized with buffers containing 250 nM digitonin with 100 μM cADPtR (magenta), cADPcR (blue), cADPR (green), or without nucleotide as control (black). Symbols indicate changes of $[Ca^{2+}]_i$ levels for 5 min, represented by the fluorescence intensity at each time (x) divided by resting intensity at time 0 (i.e., F_x/F_0). For calculations, cells with mean fluorescence intensity of 90 to 130 at time 0 were selected. $*$, Values in cells treated with cADPtR or cADPcR were significantly higher than those in control cells at $p < 0.05$. ♦, Values in cells treated with cADPtR were significantly higher than those in cells treated with cADPR at $p < 0.05$. **(d)** The graph shows concentration-dependent activity of cADPtR (magenta), cADPcR (blue) and cADPR (green) in NG108-15 cells. Symbols indicate changes of $[Ca^{2+}]_i$ levels at 280 s after membrane permeabilization, represented by fluorescence intensity at each time divided by the resting state at time 0 (i.e., F_x/F_0). Each symbol is mean ± SEM of 5 to 10 experiments. $*$, values significantly different from a drug-free control value (a gray circle) ($P < 0.05$). ♦, Values in cells treated with cADPtR were significantly higher than those in cells with cADPR at $p < 0.05$.

structure of cADPR (white) is superimposed into the three structures as shown in Figure 10(b). This crystal structure resembles the calculated cADPR and cADPtR structures, which suggests our structure determination by the molecular dynamics calculations was done relevantly.

Discussion

cAPDtR (**3**), which was designed as a stable mimic of cADPR (**1**), was successfully synthesized. In its synthesis, the key N1-β-thioribosyladenosine structure was effectively constructed by stereoselective condensation between the imidazole nucleoside derivative **8** and the 4-thioribosylamine **7** via equilibrium between the α-anomer (**7**α) and the β-anomer (**7**β). Also, the strategy using a *S*-phenyl phosphorothioate-type substrate in the intramolecular condensation reaction forming the 18-membered pyrophosphate linkage of cADPR-related compounds is demonstrated to be useful in the present case.

Although cADPR is rapidly hydrolyzed by cADPR hydrolase to give ADP-ribose under physiological conditions, cADPtR was shown to be biologically stable. Based on the X-ray crystallographic analysis of the complex of CD38 having cADPR hydrolase activity with nicotinamide guanine dinucleotide (GDP^+), Lee and Hao presented the reaction mechanism of enzymatic cADPR hydrolysis via an oxocarbenium intermediate, which is stabilized by the hydroxy group of Ser196 of the enzyme catalytic site (Liu et al., 2006). When an oxocarbenium ion, which is often an intermediate in glycosidic bond cleavage, interacts with an electronically negative nucleophilic atom such as oxygen (the hydroxyl oxygen of Ser196 in the case of CD38), it can be effectively stabilized by the adjacent ring oxygen of the sugars due to n–p^* hyperconjugation between the nonbonding orbital on the ring oxygen and the vacant p-orbital of anomeric carbon, that is known as the anomeric effect (Juaristi and Cuevas, 1992; Thatcher, 1993; Juaristi and Cuevas, 1995; Thibaudeau and Chattopadhyaya, 1999). This stereoelectronic effect would promote enzymatic and also chemical hydrolysis of cADPR at the N1-linkage.

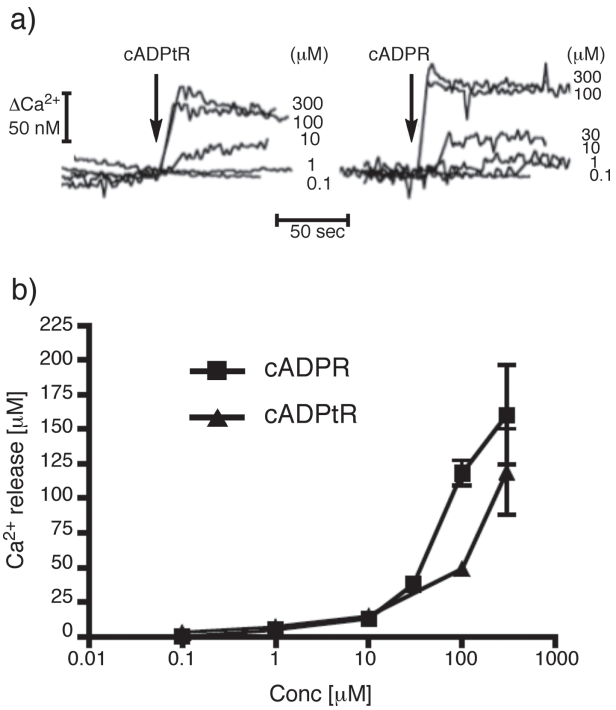

Figure 8. Effect of of cADPR (1) and cADPtR (3) on Ca^{2+} signaling in permeabilized Jurkat T cells. After addition of fura-2/free acid (1.5 mM) and charging of the intracellular Ca^{2+}-pools by the addition of ATP (1 mM) and an ATP-regenerating system consisting of creatine phosphate (10 mM) and creatine kinase (20 units/ml), the indicated concentrations of cADPR or cADP-4″-thio-ribose were added as indicated. **(a)** Representative tracings. **(b)** Data presented as mean ± SEM ($n = 2$ to 8).

On the other hand, the sulfur of thio-sugars, including thioribose, would not so effectively stabilize the corresponding thio-carbenium intermediates, because the hyperconjugation ability of sulfur is remarkably weaker than that of oxygen (Salzner and Salzner, 1993), which can be reason why cADPtR is more stable than cADPR.

On the other hand, the electron-withdrawing effect of sulfur due to its electronically negative property effectively lowered the pK_a of cADPtR, and accordingly, its pK_a is similar to that of cADPR. Under physiological pH, the population of the deprotonated imino form and the protonated amino form in cADPtR would be analogous that in cADPR. Therefore, the pK_a value of cADPtR may be favorable to exhibit its biological effects, similarly to natural messenger cADPR.

A difference of cADPcR and analog cADPtR are their pK_a values, amounting to 8.9 and 8.0, respectively. Taking the pK_a value of cADPR and the indistinguishable biological activity between cIDPR (**4**) and cADPR (Moreau et al., 2006; Huang et al., 2002; Gu et al., 2004; Xu al., 2006) in *T* cells into account, the relatively high biological activity of cADPtR might be in favour of the imino form of cADPR being the active form of the natural second messenger in *T* cells.

Our conformational analysis revealed that cADPtR has its three-dimensional structure analogous to cADPR due the similar sp^3 configuration of oxygen and sulfur bearing two non-bonding electron pairs in the N1-ribose or -thioribose ring, in which steric repulsion between the three rings (adenine, N9-ribose, and N1-ribose) seems to be minimal. Therefore, the structural and electrostatic features of cADPtR analogous to cADPR make it as biologically active as cADPR in various systems including *T*-cells, although the target proteins of cADPR in these systems is considered to be different (Kudoh et al., 2005).

Conclusion

We have successfully synthesized cADPtR (**3**) and demonstrated that it is stable and functions as cADPR (**1**) in various biological systems, i.e., sea urchin egg homogenate, neuronal cells and *T* cells. Because of the characteristic stability and high potency of cADPtR, it, as a stable equivalent of cADPR, can be useful as an effective tool for identifying target proteins and for investigating cADPR-mediated signaling pathways (Tsuzuki et al., 2013).

EXPERIMENTAL DETAILS

Chemical shifts are reported in ppm downfield from Me_4Si (^1H), MeCN (^{13}C) or H_3PO_4 (^{31}P). All of the ^1H NMR assignments described were in agreement with COSY spectra. Thin-layer chromatography was done on Merck coated plate $60F_{254}$. Silica gel chromatography was done

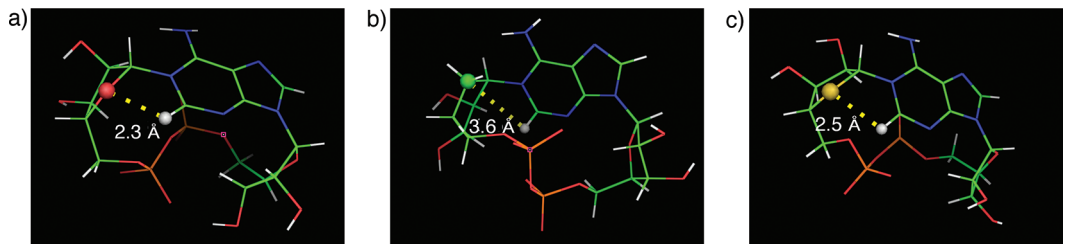

Figure 9. Structures of cADPR (a), cADPcR (b), cADPtR (c) by molecular dynamics calculations with simulated annealing method using the NOE data in D_2O. Adenine H2 (white), O4″ in cADPR (red), C6″ in cADPcR (green) and S4″ in cADPtR (yellow) are shown in sphere.

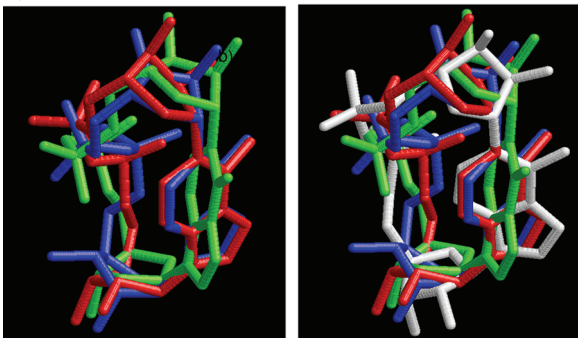

Figure 10. Superimposed displays of the structures of cADPR and its analogs. Only heavy atoms are shown. **(a)** Three caluculated structures are superimposed: cADPR (blue), cADPcR (green), and cADPtR (red). **(b)** Four structures were superimposed: The crystal structure of cADPR (white), the calculated structures of cADPR (blue), cADPcR (green), and cADPtR (red).

on Merck silica gel 5715. Reactions were carried out under an argon atmosphere.

1,4-Dideoxy-1,4-Episulfinyl-2,3-*O*-Isopropylidene-D-Ribitol (10)

To a solution of **22** (1.90 g, 10.0 mmol) in CH_2Cl_2 (30 mL) was added slowly a solution of *m*CPBA (3.18 g, 12.0 mmol) in CH_2Cl_2 (60 mL) at −78 °C, and the mixture was stirred at the same temperature for 20 min. To the mixture was added aqueous $Na_2S_2O_3$, and the resulting mixture was partitioned between EtOAc and H_2O, and the organic layer was washed with aqueous saturated $NaHCO_3$ and brine, dried (Na_2SO_4), and evaporated. The residue was purified by column chromatography (SiO_2, hexane/AcOEt = 3/1 then 1/1) to give **10** (1.88 g, 91%, white amorphous solid): ^{1}H-NMR of one isomer (500 MHz, $CDCl_3$)δ 1.33 (3 H, *s*, isopropylidene-CH_3), 1.47 (3 H, *s*, isopropylidene-CH_3), 3.29 (1 H, dd, J = 14.3, 6.3 Hz, H-1), 3.42 (1 H, ddd, J = 5.7, 5.7, 2.9 Hz, H-4), 3.45 (1 H, dd, J = 14.3, 5.7 Hz, H-1) 4.10 (1 H, dd, J = 12.6, 5.7 Hz, H-5), 4.34 (1 H, dd, J = 12.6, 2.9 Hz, H-5), 4.80 (1 H, br, OH), 5.10 (1 H, dd, J = 5.7, 3.4 Hz,

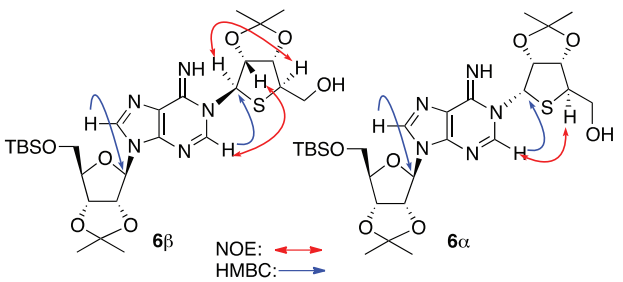

Figure 11. NOE and HMBC data of 6b and 6a.

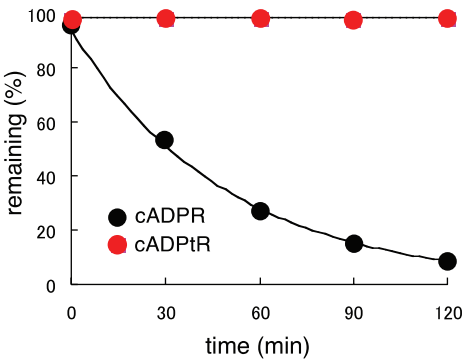

Figure 12. Stability of cADPtR and cADPR in rat brain microsome extract.

H-3), 5.20 (1 H, ddd, J = 6.3, 5.7, 3.4 Hz, H-2); ^{13}C-NMR (125 MHz, $CDCl_3$)δ 24.61, 27.12, 57.06, 57.06, 58.11, 65.63, 79.76, 82.22, 112.11; HR-MS (EI) calcd for $C_8H_{14}O_4S_2$206.06128 (M^+), found 206. 06169.

1,5-*O*-Diacetyl-2,3-*O*-Isopropylidene-4-Thio-D-Ribose (11)

A solution of **10** (135 mg, 0.44 mmol) in Ac_2O (3 mL) was heated at 100 °C for 28 h, and then evaporated. The residue was partitioned between EtOAc and H_2O, and the organic layer was washed with aqueous saturated $NaHCO_3$ and brine. The aqueous layers were combined and extracted with $CHCl_3$. The organic layers were combined, dried (Na_2SO_4), and evaporated. The residue was purified by column chromatography (SiO_2, hexane/AcOEt = 6/1, 3/1 then 1/1) to give **11** (93 mg, 64%, J = 11.5, 5.7 Hz, H-5), 4.89–4.91 (2 H, m, H-2, H-3), 6.04 (1 H, *s*, H-1), for α-anomer, δ 1.36 (3 H, *s*, isopropylidene-CH_3), 1.54 (3 H, *s*, isopropylidene-CH_3), 2.10 (3 H, *s*, Ac), 2.15 (3 H, *s*, Ac), 3.90 (1 H, m, H-4), 4.19 (1 H, dd, J = 11.5, 6.3 Hz, H-5), 4.35 (J = 11.5, 5.7 Hz, H-5), 4.89–4.91 (2 H, m, H-2, H-3), 6.04 (1 H, *s*, H-1), for α-anomer, δ 1.36 (3 H, *s*, isopropylidene-CH_3), 1.54 (3 H, *s*, isopropylidene-CH_3), 2.10 (3 H, *s*, Ac), 2.15 (3 H, *s*, Ac), 3.90 (1 H, m, H-4), 4.19 (1 H, dd, J = 11.5, 6.3 Hz, H-5), 4.35 (1 H, dd, J = 11.5, 6.3 Hz, H-5), 4.67 (1 H, dd, J = 6.3, 4.0 Hz, H-3), 4.88 (1 H, m, H-2), 6.09 (1 H, d, J = 5.2 Hz, H-1) ^{13}C-NMR (100 MHz, $CDCl_3$)δ 20.85, 21.21, 24.61, 26.38, 53.85, 65.71, 85.13, 87.17, 88.54, 111.29, 169.16, 170.49; HR-MS (FAB, positive) calcd for $C_{12}H_{18}NaO_6S$ 313.0722 [(M+Na)$^+$], found 313.0717.

5-*O*-Acetyl-2,3-*O*-Isopropylidene-4-Thio-β-D-Ribofuranosylazide (12)

To a solution of **11** (2.26 g, 7.78 mmol) and $TMSN_3$ (3.09 mL, 23.3 mmol) in CH_2Cl_2 (20 mL) was added a solution of $SnCl_4$ (223 mL, 1.91 mmol) in CH_2Cl_2 (10 mL) at 0 °C, and the mixture was stirred at the

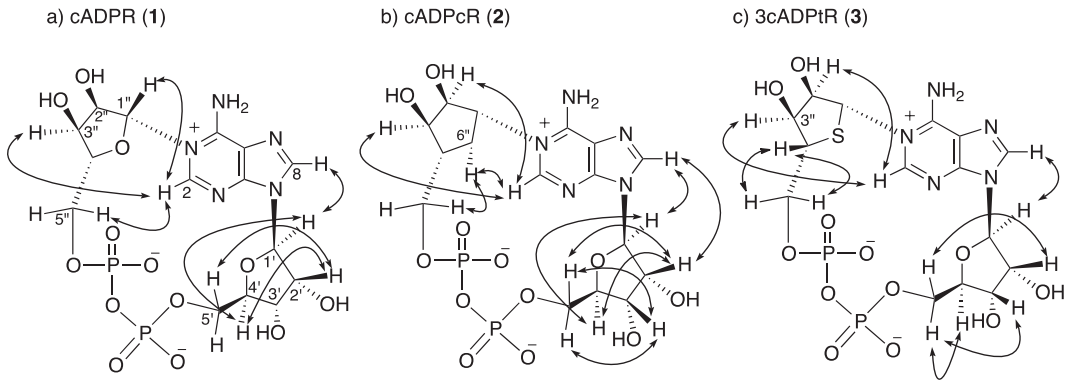

Figure 13. **Important correlations in NOESY spectra of (a) cADPR (1), (b) cADPcR (2), (c) cADPtR (3), used for the calculations.**

same temperature for 5 min. To the mixture was added aqueous saturated $NaHCO_3$, and the resulting white precipitate was filtered off with Celite. The filtrate was washed with aqueous saturated $NaHCO_3$ and brine, dried (Na_2SO_4), and evaporated. The residue was purified by column chromatography (SiO_2, hexane/AcOEt = 20/1) to give **12** (1.84 g, 86%, yellow oil): ^{1}H-NMR (400 MHz, $CDCl_3$)δ 1.31 (3 H, *s*, isopropylidene-CH_3), 1.50 (3 H, *s*, isopropylidene-CH_3), 2.11 (3 H, *s*, Ac), 3.63 (1 H, dd, J = 10.0, 5.4 Hz, H-4), 4.12 (1 H, dd, J = 11.3, 10.0 Hz, H-5), 4.27 (1 H, dd, J = 11.3, 5.4 Hz, H-5), 4.64 (1 H, d, J = 5.4 Hz, H-3), 4.86 (1 H, d, J = 5.4 Hz, H-2), 5.18 (1 H, *s*, H-1); ^{13}C-NMR (100 MHz, $CDCl_3$)δ 20.73, 24.51, 26.26, 54.29, 65.21, 76.13, 85.59 89.06, 111.23, 170.40; HR-MS (FAB, positive) calcd for $C_{10}H_{15}N_3NaO_4S$ 296.0681 [(M+H)$^+$], found 296.0695.

2,3-*O*-Isopropylidene-4-Thio-D-Ribofuranosylamine (7)

A mixture of **12** (1.25 g, 4.57 mmol) and Pd/C (10%, 630 mg) in MeOH (45 mL) was stirred under atmospheric pressure of H_2 at room temperature for 1 h, and then the catalysts were filtered off with Celite. The filtrate was evaporated, and the residue was purified by column chromatography (NH-silica gel, hexane/AcOEt = 6/1, 2/1 then 1/3) to give **7** (1.09 g, quant., α/β = 1/2, brown oil): ^{1}H-NMR (500 MHz, $CDCl_3$)δ 1.30 (2 H, *s*), 1.36 (1 H, *s*), 1.52, (2 H, *s*), 1.57 (1 H, *s*), 1.83 (2 H, brs), 3.58 (2/3 H, dd, J = 7.7, 5.4 Hz), 3.73 (1/3 H, ddd, J = 6.3, 5.9 Hz), 4.32 (2/3 H, dd, J = 11.7, 7.7 Hz), 4.43 (2/31 H, dd, J = 11.7, 5.4 Hz), 4.49 (1/3 H, dd, J = 11.3, 5.9 Hz), 4.60–4.66 (2/3 H, m), 4.71–4.74 (1 H, m), 4.79 (2/3 H, d, J = 5.2 Hz, b–H–1), 4.92 (1/3 H, dd, J = 4.5 Hz), 5.04 (2/3 H, d, J = 4.5 Hz); ^{13}C-NMR (100 MHz, $CDCl_3$)δ −5.64, −5.51, 18.23, 24.36, 25.27, 25.80, 26.50, 27.22, 57.20, 63.68, 64.31, 64.63, 81.06, 85.99, 86.45, 87.57, 91.20, 91.65, 95.13, 110.33, 113.74, 117.26, 132.20, 148.52, 151.04; HR-MS (EI) calcd for $C_8H_{15}NO_3S$ 205.0773 (M$^+$), found 205.0773.

*N*1-(2,3-*O*-isopropylidene-4-thio-β-D-ribofuranosyl)-5″-*O*-(*tert*-butyldimethylsilyl)-2′,3′-*O*-Isopropylideneadenosine (6β)

A solution of **7** (381 mg, 1.87 mmol) and **8** (1.79 g, 4.00 mmol) in MeOH (10 mL) was stirred at room temperature for 10 h, and then evaporated. The residue was purified by flash column chromatography (silica gel, hexane/AcOEt = 1/2, AcOEt , then AcOEt/MeOH = 9/1) to give **6β** (700 mg, 61%, white amorphous solid), **6α** (59 mg, 5%, white amorphous solid), **14** (30 mg, 4%, yellow amorphous solid). **6β**: ^{1}H-NMR (500 MHz, CDCl)δ 0.04 (3 H, *s*, Si-CH_3), 0.05 (3 H, *s*, Si-CH_3), 0.86 (9H, *s*, *tert*-butyl), 1.35 (3 H, *s*, isopropylidene-CH_3), 1.39 (3 H, *s*, isopropylidene-CH_3), 1.61 (3 H, *s*, isopropylidene-CH_3), 1.63 (3 H, *s*, isopropylidene-CH_3), 3.77 (1 H, dd, J = 11.4, 4.0, 4.0 Hz, H-5′), 3.83–3.88 (2 H, m, H-5′, H-5″), 3.90 (1 H, m, H-4″), 4.01 (1 H, dd, J = 11.4, 3.7 Hz, H-5″), 4.39 (1 H, m, H-4′), 4.88 (1 H, dd, J = 6.3, 3.4 Hz, H-3′), 4.99 (1 H, dd, J = 5.2, 1.7 Hz, H-3″), 5.06 (1 H, dd, J = 6.3, 2.3 Hz, H-2′), 5.51 (1 H, dd, J = 5.2, 3.4 Hz, H-2″), 6.00 (1 H, d, J = 3.4 Hz, H-1″), 6.02 (1 H, d, J = 2.3 Hz, H-1′), 7.85 (1 H, *s*, H-8), 7.88 (1 H, *s*, H-2); ^{13}C-NMR (125 MHz, $CDCl_3$)δ −5.58, −5.47, 18.25 25.25, 25.80, 27.13, 27.92, 55.53, 63.37, 64.75, 74.54, 81.19, 85.23, 85.75, 86.22, 86.95, 91.15, 111.66, 114.09, 123.75, 137.20, 140.30, 146.81, 153.31; UV (MeOH) λ_{max} = 260 nm; LR-MS (FAB, positive) m/z 610 [(M+H)$^+$]; Anal. Calcd for $C_{27}H_{43}N_5O_7SSi$: C, 53.18; H, 7.11, N, 11.48. Found C, 52.88; H, 6.95; N, 11.35; NOE irradiated H-2/ observed H-2″ (3.8%), irradiated H-1″/observed H-4″ (2.3%), irradiated H-2″/ observed H-2 (4.7%), irradiated H-4″/ observed H-1″ (3.2%). **6α**: ^{1}H-NMR (500 MHz, CDCl)δ 0.05 (3 H, *s*, Si-CH_3), 0.05 (3 H, *s*, Si-CH_3), 0.87 (9H, *s*, *tert*-butyl), 1.35 (3 H, *s*, isopropylidene-CH_3), 1.39 (3 H, *s*, isopropylidene-CH_3), 1.61 (3 H, *s*, isopropylidene-CH_3), 1.63 (3 H, *s*, isopropylidene-CH_3), 3.56 (1 H, d, J = 4.1, 4.1 Hz, H-4″), 3.76 (1 H, dd, J = 11.3, 3.6 Hz, H-5′), 3.84–3.88 (2 H, m, H-5′, H-5″), 3.93 (1 H, dd, J = 10.9, 4.1 Hz, H-5″), 4.39 (1 H, ddd, J = 6.3, 3.6, 3.6 Hz, H-4′), 4.90 (1 H, dd, J = 6.3, 2.7 Hz, H-3′),

4.95 (1 H, d, $J = 5.9$ Hz, H-3″), 5.01 (1 H, dd, $J = 5.9$, 4.5 Hz, H-2″), 5.09 (1 H, dd, $J = 6.3$, 2.7 Hz, H-2′), 6.05 (1 H, d, $J = 2.7$ Hz, H-1′), 7.02 (1 H, d, $J = 4.5$ Hz, H-1″), 7.83 (1 H, *s*, H-8), 8.42 (1 H, *s*, H-2); ^{13}C-NMR (125 MHz, $CDCl_3$)δ −5.54, −5.44, 18.29, 24.22, 25.33, 25.83, 25.97, 27.16, 54.36, 61.15, 63.34, 65.17, 80.59, 81.19, 85.30, 85.87, 86.99, 91.16, 111.38, 114.09, 122.77, 136.83, 140.88, 147.76, 155.00; UV (MeOH) λ_{max} = 259 nm; HR-MS (FAB, positive) calcd for $C_{28}H_{43}N_5O_7SSi$ 610.2731 (MH^+), found 610.2727. NOE irradiated H-2/observed H-4″ (1.0%), irradiated H-1″/observed H-2″ (10.7%), irradiated H-2″/observed H-1″ (8.4%), irradiated H-4″/observed H-2 (1.7%). **13**: ^{1}H-NMR (500 MHz, $CDCl_3$) δ 0.00 (3 H, *s*, Si–CH_3), 0.01 (3 H, *s*, Si–CH_3), 0.83 (9H, *s*, *tert*-butyl), 1.32 (3 H, *s*, isopropylidene-CH_3), 1.40 (3 H, *s*, isopropylidene-CH_3), 1.59 (3 H, *s*, isopropylidene-CH_3), 1.62 (3 H, *s*, isopropylidene-CH_3), 3.69 (1 H, m, H-4″), 3.73 (1 H, dd, $J = 11.3$, 4.5 Hz, H-5′), 3.83–3.87 (2 H, m, H-5′, H-5″), 3.90 (1 H, br, OH), 4.07 (1 H, dd, $J = 10.4$, 2.7 Hz, H-5″), 4.39 (1 H, m, H-4′), 4.87 (1 H, d, $J = 5.0$ Hz, H-2′), 4.94–4.96 (2 H, m, H-3′, H-3″), 5.28 (1 H, dd, $J = 6.3$, 2.3 Hz, H-2′), 6.13 (1 H, d, $J = 2.3$ Hz, H-1′), 6.16 (1 H, br, H-1″), 7.49 (1 H, d, $J = 9.1$ Hz, NH), 7.97 (1 H, *s*, H-2), 8.45 (1 H, *s*, H-8); ^{13}C-NMR (125 MHz, $CDCl_3$)δ −5.64, −5.51, 18.23, 24.36, 25.27, 25.80, 26.50, 27.22, 57.20, 63.68, 64.31, 64.63, 81.06, 85.99, 86.45, 87.57, 91.20, 91.65, 95.13, 110.33, 113.74, 117.26, 132.20, 148.52, 151.04; UV (MeOH) λ_{max} = 273 nm; HR-MS (FAB, positive) calcd for $C_{27}H_{44}N_5O_7SSi$ 610.2731 (MH^+), found 610.2741.

*N*1-(2,3-*O*-isopropylidene-4-thio-5-*O*-dimethoxytrityl-*β*-D-ribofuranosyl)-5′-*O*-(*tert*-butyldimethylsilyl)-2′,3′-*O*-Isopropylideneadenosine (14)

A solution of **6***β* (889 mg, 1.46 mmol) and DMTrCl (989 mg, 2.92 mol) in pyridine (5 mL) was stirred at room temperature for 12 h. After addition of MeOH, the resulting mixture was partitioned between EtOAc and 1 M aqueous HCl, and the organic layer was washed with H_2O and brine, dried (Na_2SO_4), and evaporated. The residue was purified by column chromatography (silica gel, hexane/AcOEt = 6/1, 3/1, 3/2, and 2/3) to give **14** (1.08 g, 81%, white amorphous solid): ^{1}H-NMR (500 MHz, $CDCl_3$)δ 0.05 (3 H, *s*, Si–CH_3), 0.06 (3 H, *s*, Si–CH_3), 0.88 (9H, *s*, *tert*-butyl), 1.30 (3 H, *s*, isopropylidene-CH_3), 1.38 (3 H, *s*, isopropylidene-CH_3), 1.59 (3 H, *s*, isopropylidene-CH_3), 1.62 (3 H, *s*, isopropylidene-CH_3), 3.40–3.46 (2 H, m, H-5″ × 2), 3.77 (1 H, m, H-5′), 3.78 (3 H, *s*, OCH_3), 3.78 (3Hy, s, OCH_3), 3.80–3.85 (2 H, m, H-4″, H-5′), 4.38 (1 H, ddd, J = 5.7, 4.0, 4.0 Hz, H-4′), 4.72 (1 H, dd, $J = 5.7$, 4.0 Hz, H-3″), 4.86 (1 H, dd, $J = 6.3$, 5.7 Hz, H-3′), 4.89 (1 H, dd, $J = 5.7$, 2.3 Hz, H-2″), 4.97 (1 H, dd, $J = 6.3$, 2.9 Hz, H-2′) 6.02 (1 H, d, $J = 2.9$ Hz, H-1′), 6.52 (1 H, d, $J = 2.3$ Hz, H-1″), 6.81–7.47 (13 H, m, Ar), 7.82 (1 H, *s*, H-8), 8.12 (1 H, *s*, H-2); ^{13}C-NMR (125 MHz, $CDCl_3$)δ −5.58, −5.47, 18.22, 25.21, 25.28, 25.79, 27.13, 27.35, 54.95, 55.05, 63.30, 64.85, 66.78, 81.06, 84.82, 85.25, 86.53, 86.79, 89.22, 90.86, 112.38, 113.03, 113.05, 114.01, 123.23, 126.66, 127.73, 127.95, 129.92, 129.96, 135.46, 135.60, 136.51, 140.35, 144.47, 145.55, 153.98, 158. 37; LR-MS (FAB, positive) m/z 882 [$(M+H)^+$]; UV (MeOH) λ_{max} = 259 nm; Anal. Calcd for $C_{48}H_{61}N_5O_9SSi$: C, 63.20; H, 6.74, N, 7.68. Found C, 63.19; H, 6.91; N, 7.39.

*N*1-(2,3-*O*-isopropylidene-4-thio-5-*O*-dimethoxytrityl-*β*-D-ribofuranosyl)-2′,3′-*O*-Isopropylideneadenosine (15)

A solution of **14** (94 mg, 103 mmol), TBAF (1.0 M in THF, 200 mL, 0.20 mmol) and AcOH (6 μL, 1 μmol) in THF (800 mL) was stirred at room temperature for 9 h, and then evaporated. The residue was purified by column chromatography (silica gel, hexane/AcOEt = 2/1, /1, 3/2, and 1/3) to give **15** (83 mg, quant., colorless amorphous solid): ^{1}H-NMR (500 MHz, $CDCl_3$)δ 1.29 (3 H, *s*, isopropylidene), 1.37 (3 H, *s*, isopropylidene), 1.58 (3 H, *s*, isopropylidene), 1.63 (3 H, *s*, isopropylidene), 3.40 (1 H, dd, $J = 9.7$, 6.9 Hz, H-5″), 3.46 (1 H, dd, $J = 9.7$, 6.9 Hz, H-5″), 3.72 (1 H, dd, $J = 12.6$, 10.9 Hz, H-5″), 3.77 (3 H, *s*, OCH_3), 3.77 (3 H, *s*, OCH_3), 3.79 (1 H, m, H-4″), 3.86 (1 H, d, $J = 12.6$ Hz, H-5′), 4.47 (1 H, m, H-4′), 4.67 (1 H, dd, $J = 5.7$ 4.0 Hz, H-3″), 4.84 (1 H, dd, J = 5.7, 2.3 Hz, H-2″), 4.99–5.03 (2 H, m, H-2′, H-3′), 5.31 (1 H, d, $J = 10.9$ Hz, OH), 5.75 (1 H, d, $J = 4.6$ Hz, H-1′), 6.44 (1 H, d, $J = 2.3$ Hz, H-1″), 6.80–7.42 (13Hy, m, Ar), 7.57 (1 H, br s, NH), 7.63 (1 H, *s*, H-8), 8.14 (1 H, *s*, H-2); ^{13}C-NMR (125 MHz, $CDCl_3$)δ 25.42, 25.48, 27.60, 27.76, 54.98, 55.39, 63.28, 65.05, 67.35, 81.62, 83.90, 84.89, 86.03, 86.90, 89.28, 93.95, 112.90, 113.35, 114.39, 125.04, 127.03, 128.07, 128.26, 130.18, 130.23, 135.74, 135.92, 138.32, 139.63, 144.66, 146.01, 153.86, 158.70; UV (MeOH) λ_{max} = 258 nm; HR-MS (FAB, positive) calcd for $C_{42}H_{48}N_5O_9S$ 798.3173 [$(M+H)^+$], found 798.3193.

*N*1-(2,3-*O*-isopropylidene-4-thio-5-*O*-dimethoxytrityl-*β*-D-ribofuranosyl)-5′-*O*-[bis(phenylthio)phosphoryl]-2′,3′-*O*-Isopropylideneadenosine (16)

To a solution of **15** (845 mg, 1.06 mmol) in pyridine (5 mL) was added a solution of PSS (809 mg, 2.12 mmol) and TPSCl (693 mg, 1.91 mmol) in pyridine (5 mL) at −15 °C, and the mixture was stirred at the same temperature for 2.5 h. After addition of H_2O, the resulting mixture was partitioned between EtOAc and 1 M aqueous HCl, and the organic layer was washed with H_2O and brine,

dried (Na_2SO_4), and evaporated. The residue was purified by column chromatography (silica gel, hexane/AcOEt = 3/1, 1/1, 1/2, and 1/3) to give **16** (812 mg, 72%, white amorphous solid): ^{1}H-NMR (500 MHz, $CDCl_3$)δ 1.25 (3 H, *s*, isopropylidene-CH_3), 1.36 (3 H, *s*, isopropylidene-CH_3), 1.57 (3 H, *s*, isopropylidene-CH_3), 1.61 (3 H, *s*, isopropylidene-CH_3), 3.40 (1 H, m, H-5′), 3.46 (1 H, dd, J = 9.2, 5.7 Hz, H-5′), 3.77 (3 H, *s*, OCH_3), 3.77 (3 H, *s*, OCH_3), 3.79 (1 H, m, H-4″), 4.37–4.39 (2 H, m, H-5″ × 2), 4.44 (1 H, m, H-4′), 4.64 (1 H, m, H-3″), 4.83 (1 H, dd, J = 6.3, 2.3 Hz, H-2″), 4.89 (1 H, dd, J = 6.3, 3.4 Hz, H-3′), 5.06 (1 H, dd, J = 6.3, 2.3 Hz, H-2′), 5.97 (1 H, d, J = 2.3 Hz, H-1′), 6.55 (1 H, d, J = 2.3 Hz, H-1″), 6.80–7.48 (23 H, m, Ar), 7.82 (1 H, *s*, H-8), 8.09 (1 H, *s*, H-2); ^{13}C-NMR (125 MHz, $CDCl_3$)δ 25.32, 27.14, 27.48, 55.09, 55.19, 64.99, 66.14, 66.33, 66.39, 80.89, 84.44, 84.70, 84.79, 86.58, 89.09, 90.62, 112.59, 113.12, 113.15, 123.71, 125.67, 125.71, 125.73, 125.76, 126.79, 127.85, 128.10, 129.42, 129.44, 129.63, 129.66, 129.68, 129.70, 130.03, 130.08, 135.11, 135.16, 135.27, 135.31, 135.58, 135.71, 137.27, 140.28, 144.55, 145.85, 153.96, 158.47; ^{31}P-NMR (202 MHz, $CDCl_3$) d 50.79 (s); UV (MeOH) λ_{max} = 258 nm; HR-MS (FAB, positive) calcd for $C_{54}H_{57}N_5O_{10}PS_3$ 1062.3005 [(M+H)$^+$], found 1062.2999.

*N*1-(2,3-*O*-isopropylidene-4-thio-β-D-ribofuranosyl)-5′-*O*-[bis(phenylthio)phosphoryl]-2′,3′-*O*-Isopropylideneadenosine (17)

A solution of **16** (23 mg, 22 mmol) in aqueous 60% AcOH (2 mL) was stirred at room temperature for 4 h, and then evaporated. The residue was purified by column chromatography (silica gel, hexane/AcOEt = 1/1, 1/3, then AcOEt) to give **17** (15 mg, colorless amorphous solid): ^{1}H-NMR (500 MHz, $CDCl_3$)δ 1.34 (3 H, *s*, isopropylidene-CH_3), 1.38 (3 H, *s*, isopropylidene-CH_3), 1.60 (3 H, *s*, isopropylidene-CH_3), 1.62 (3 H, s, isopropylidene-CH_3), 3.76–3.83 (3 H, m, H-4″, H-5″ × 2), 4.30 (1 H, ddd, J = 11.4, 9.7, 5.2 Hz, H-5′), 4.43 (1 H, ddd, J = 6.3, 5.2, 2.9 Hz, H-4′), 4.47 (ddd, 1 H, J = 12.6, 9.7, 6.3 Hz, H-5′), 4.83 (1 H, d, J = 5.2 Hz, H-3″), 5.04 (1 H, dd, J = 6.3, 2.9 Hz, H-3′), 5.09 (1 H, dd, J = 5.2, 1.1 Hz, H-2″) 5.28 (1 H, dd, J = 6.3, 1.7 Hz, H-2′), 5.98 (1 H, d, J = 1.7 Hz, H-1′), 6.07 (1 H, d, J = 1.1 Hz, H-1″), 7.27–7.54 (10H, m, Ar), 7.63 (1 H, *s*, H-8), 8.55 (1 H, *s*, H-2); ^{13}C-NMR (125 MHz, $CDCl_3$) d 24.88, 25.08, 26.87, 27.28, 57.09, 64.26, 66.26, 66.32, 73.96, 81.93, 84.52, 85.65, 85.73, 85.93, 89.68, 91.39, 110.99, 114.10, 123.84, 125.28, 125.34, 125.46, 125.52, 129.27, 129.29, 129.38, 129.40, 129.58, 129.60, 129.73, 129.75, 135.04, 135.09, 135.37, 135.40, 138.01, 140.22, 147.09, 154.09; ^{31}P-NMR (202 MHz, $CDCl_3$) d 52.23 (s); UV (MeOH) λ_{max} = 251, 258 nm; HR-MS (FAB, positive) calcd for $C_{33}H_{39}N_5O_8PS_3$ 760.1698 [(M+H)$^+$], found 760.1710.

*N*1-(2,3-*O*-isopropylidene-4-thio-5-*O*-phospholyl-β-D-ribofuranosyl)-5′-*O*-(phenylthiophosphoryl)-2′,3′-*O*-Isopropylideneadenosine (5)

A solution of $MeOPOCl_2$ (30 mL, 0.30 mmol) in pyridine (1 mL) was stirred at −15 °C for 15 min. To the solution was added a solution of **17** (75 mg, 0.10 mol) in pyridine (1 mL), and the mixture was stirred at the same temperature for 2 h. To the resulting solution was added triethylammonium acetate (TEAA) buffer (0.5 M, pH 7.0, 3 mL) then H_3PO_2 (101 μL, 2.0 mmol) and Et_3N (140 μL, 1.0 mmol), and the mixture was stirred at room temperature for 13 h, and then evaporated. The residue was partitioned between EtOAc and H_2O, and the aqueous layer was evaporated. The residue was purified by column chromatography (ODS, 1.2 × 16 cm, 0–37% CH_3CN/0.1 M TEAA buffer (0.1 M, pH 7.0, 400 mL), linear gradient). The excess TEAA included in the residue was removed by column chromatography (ODS, 1.2 × 16 cm, CH_3CN/H_2O = 1/1). The product was lyophilized to give **5** (37 mg, 512 OD_{260} unit, 46%) as a triethylammonium salt: ^{1}H-NMR (500 MHz, D_2O)δ 1.26 (9H, t, J = 7.4 Hz ($CH_3CH_2)_3N$), 1.40 (3 H, *s*, isopropylidene-CH_3), 1.43 (3Hy, s, isopropylidene-CH_3), 1.63 (3 H, *s*, isopropylidene-CH_3), 1.69 (3Hy, s, isopropylidene-CH_3), 3.18 (6H, q, J = 7.4 Hz, ($CH_3CH_2)_3N$), 4.10–4.13 (4H, m, H-4″, H-5′ × 2, H-5″), 4.70 (1 H, m, H-4″), 4.20 (1 H, m, H-5′), 4.22 (1 H, m, H-5″), 4.32 (1 H, m, H-5″), 4.71 (1 H, m, H-4′), 4.94 (1 H, d, J = 5.2 Hz, H-3′) 5.12–5.15 (2 H, m, H-2″, H-3″), 5.42 (1 H, dd, J = 6.3, 2.9 Hz, H-3′), 5.39 (1 H, d, J = 5.2 Hz, H-2′), 5.95 (1 H, *s*, H-1″), 6.37 (1 H, *s*, H-1′), 7.19–7.33 (5H, m, Ar), 8.41 (1 H, *s*, 8-H), 9.24 (1 H, *s*, 2-H); ^{13}C-NMR (125 MHz, D_2O)δ 8.30, 24.32, 24.35, 25.95, 26.41, 46.71, 54.48, 54.55, 65.90, 65.95, 66.59, 66.62, 75.84, 81.39, 84.11, 86.19, 86.27, 86.52, 89.30, 90.88, 113.51, 114.72, 119.08, 127.91, 129.08, 129.47, 129.51, 132.75, 132.79, 143.02, 145.48, 146.84, 150.53; ^{31}P-NMR (202 MHz, D_2O) d 17.54 (s), 0.80 (s); UV (D_2O) λ_{max} = 258 nm; HR-MS (FAB, negative) calcd for $C_{27}H_{34}N_5O_{12}P_2S_2$746.1126 [(M-H)$^-$], found 746.1106.

Cyclic ADP-4-Thio-Ribose 2′,3′-, 2″,3″-Bisacetonide (19)

To a mixture of $AgNO_3$ (36 mg, 0.21 mmol), Et_3N (29 ml, 0.21 mmol), and MS 3A (powder, 1.0 g) in pyridine (8 mL), a solution of **5** (9 mg, 50 OD_{260} unit, 4 mmol) in pyridine (8 mL) was added slowly over 15 h, using a syringe-pump, at room temperature under shading. To the mixture was added TEAA buffer (2.0 M, pH 7.0, 2 mL), and the resulting mixture was filtered with Celite and evaporated. The residue was partitioned between EtOAc and H_2O, and the aqueous layer was evaporated, and the residue was purified by column chromatography (ODS, 1.2 × 16 cm, 0–35% CH_3CN/0.1 M

TEAA buffer (0.1 M, pH 7.0, 400 mL), linear gradient). The excess TEAA included in the residue was removed by column chromatography (ODS, 1.2 × 16 cm, $CH_3CN/H_2O = 1/1$). The product was lyophilized to give **19** (6 mg, 36 OD_{260} unit, 72%) as a triethylammonium salt: ^{1}H-NMR (500 MHz, D_2O)δ 1.24 (9H, t, $J = 7.4$ Hz ($CH_3CH_2)_3N$), 1.41 (3 H, *s*, isopropylidene-CH_3), 1.43 (3 H, *s*, isopropylidene-CH_3), 1.61 (3 H, *s*, isopropylidene-CH_3), 1.65 (3 H, s, isopropylidene-CH_3), 3.17 (6H, q, $J =$ 7.4 Hz, ($CH_3CH_2)_3N$), 3.91 (1 H, m, H-5′), 4.13 (1 H, m, H-4″), 4.20 (1 H, m, H-5′), 4.22 (1 H, m, H-5″), 4.32 (1 H, m, H-5″), 4.58 (1 H, m, H-4′), 5.07 (1 H, d, $J = 4.8$ Hz, H-3″) 5.13 (1 H, d, $J = 4.8$ Hz, H-2″), 5.42 (1 H, dd, $J = 6.3$, 2.9 Hz, H-3′), 5.89 (1 H, dd, $J = 6.3$, 1.7 Hz, H-2′), 5.99 (1 H, *s*, H-1″), 6.38 (1 H, d, $J =$ 1.7 Hz, H-1′), 8.38 (1 H, *s*, 8-H), 9.59 (1 H, s, 2-H); ^{13}C-NMR (125 MHz, D_2O)δ 8.29, 24.39, 24.42, 26.07, 26.26, 46.73, 55.40, 55.49, 64.80, 68.03, 64.83, 68.00, 77.65, 81.36, 83.25, 86.65, 86.73, 87.34, 90.82, 91.45, 113.11, 114.59, 119.58, 144.91, 145.55, 147.20, 150.67; ^{31}P-NMR (202 MHz, D_2O) d −10.62 (d, $J = 15.5$ Hz), d −11.29 (d, $J = 15.5$ Hz); UV (D_2O) $\lambda_{max} = 258$ nm; HR-MS (FAB, negative) calcd for $C_{21}H_{28}N_5O_{12}P_2S$ 636.0936 [(M-H)$^-$], found 636.0947.

Cyclic ADP-4-Thio-Ribose (3)

A solution of **19** (280 OD_{260} unit, 25 mmol) in aqueous 60% HCO_2H (1 mL) was stirred at room temperature for 40 h and then evaporated. After co-evaporation with H_2O, the residue was purified by column chromatography (ODS, 1.2 × 16 cm, TEAA buffer (5 mM, pH 7.0)). The excess TEAA included in the residue was removed by column chromatography (Sephadex LH 20, 2.5 × 20 cm, H_2O) to give **3** as a triethylammonium salt, which was converted into a free acid form by passing through columns of Daiaion PK212L (H^+ form, 0.7 cm × 5 cm, H_2O). The free acid was passed throuh Chelex 100 column (K^+ form, 0.7 cm × 6 cm, H_2O). The eluent was evapolated and lyophilized to give **3** (138 OD_{260} unit, 49%) as a potassium salt. **3** (potassium salt): ^{1}H-NMR (500 MHz, D_2O) δ 3.59 (1 H, dd, $J = 8.2$, 3.2 Hz), 4.08 (1 H, m), 4.19 (1 H, m), 4.24–4.36 (4H, m), 4.52 (1 H, ddd $J = 10.4$, 8.2, 2.7 Hz), 4.60 (1 H, dd, $J = 5.4$, 2.3 Hz), 5.18 (1 H, dd, $J = 5.9$, 5.4 Hz), 5.87 (2 H, m), 7.97 (1 H, s), 9.25 (1 H, s); ^{13}C-NMR (125 MHz, D_2O)δ 50.8, 50.9, 63.1, 65.0, 65.0, 70.1, 70.6, 72.6, 73.0, 78.3, 84.7, 84.8, 90.5, 120.0, 145.3, 145.9, 146.9, 150.8; ^{31}P-NMR (162 MHz, D_2O)δ −9.15 (d, $J = 12.2$ Hz), δ −10.20 (d, $J = 12.2$ Hz); UV (D_2O) $\lambda_{max} = 258$ nm; HR-MS (FAB, negative) calcd for $C_{15}H_{20}N_5O_{12}P_2S$ 556.0304 [(M-H)$^-$], found 556.2994. **3** (free acid): ^{1}H-NMR (500 MHz, D_2O)δ 3.72 (1 H, ddd, $J = 5.2$, 3.4, 1.7 Hz), 4.09 (1 H, ddd, $J = 10.9$, 6.9, 2.9 Hz), 4.25 (1 H, ddd, $J = 11.5$, 5.2, 2.3 Hz), 4.35–4.39 (3 Hy, m), 4.51 (1 H, ddd, $J = 10.9$, 7.4, 4.0 Hz), 4.53 (1 H, dd, $J = 5.9$, 2.9 Hz), 4.71 (1 H, dd, $J = 5.2$, 2.3 Hz), 5.22 (1 H, dd, $J = 6.3$, 5.2 Hz), 5.97 (1 H, d, $J = 2.9$ Hz), 6.04 (1 H, d, $J = 6.3$ Hz), 8.38 (1 H, s), 9.90 (1 H, s).

Stability in Rat Brain Microsomes

Rat brain microsomes were prepared by a procedure according to the previous method (Murayama, T. and Ogawa Y. (1996). *J. Biol. Chem.* 271, 5079–5084.). cADPR or cADPtR (1.6 OD_{260} unit) was preincubated in 20 mM MOPS buffer (pH 7.1, 160 μL) at 37 °C for 5 min. This was added to the solution of the microsome fraction of rat brain extract (14.9 mg/mL, 140 μL), and the mixture was incubated at 37 °C. The reaction mixture was sampled (25 μL) at every 30 min afterwards and diluted with water (175 μL), which was frozen in liquid nitrogen to stop the reaction. After the samples were a centrifuged at 12000 rpm at 4 °C for 15 min, the supernatants were filtered using centrifugal filter at 12000 rpm at 4 °C for 15 min, and the resulting filtrates (70 μL) were analyzed by ion exchange HPLC (TSK-GEL DEAE-2SW, 4.6 × 250 mm; 5–35% 1 M HCO_2NH_4/20% MeCN, 20 min; 260 nm). The results are shown in Figure 2.

Biological Evaluations with Sea Urchin Egg Homogenate or *T*-cells

These bioassays were carried out as reported previously (Kudoh et al., 2005).

Biological Evaluations with Neuronal Cultured Cells

NG108-15 neuroblastoma *x* glioma hybrid cells were cultured as reported previously (Higashida et al., 1990). Oregon Geen-loaded NG108-15 cells were incubated for 2 min in the following calcium-free medium (140 mM *K*-glutamate, 20 mM PIPES, 5 mM EGTA, 2 mM Mg-ATP, 10 mM glucose, 1 mM magnesium chloride, 0.01% bovine serum albumin, pH 6.8) at 37 °C, and subsequently permeabilized with 250 nM digitonin in the calcium-free medium. cADPR (1–100 μM), cADPcR (1–100 μM), or cADPcR (1–100 μM) were applied together with the digitonin-containing permeabilization buffer to be allowed free passage of these nucleotides into the cytoplasm. Concentrations of $[Ca^{2+}]_i$ were determined microspectrofluorometrically using fura-2 in differentiated NG108-15 cells cultured on polylysine-coated glass coverslips. The cells were loaded with fura-2 using 5 μM Oregon Green 488 1,2-bis(2-aminophenoxy)ethane-*N*,*N*,*N*,*N*-tetraacetate acetoxymethylester (BAPTA-1 AM). Fluorescence was measured at 37 °C with excitation wavelengths of 485 nm and emission wavelengths of 538 nm using an Argus 50 Ca^{2+} microspectrofluorometric system (Hamamatsu Photonics, Hamamatsu, Japan) and images were collected every 10 s for up to 5 min.

The changes in fluorescence intensity of each cell were expanded into an X-t plane, and data were performed in fluorescence intensity at each time (x) divided by resting intensity at time 0, i.e., F_x/F_0 (Amina et al., 2010). Data are expressed as mean ± s.e.m. Statistical analysis was performed using a Student's t test. The criterion for significance in all cases was $p < 0.05$.

Computational Calculations

For structure determination, molecular calculations were carried out by AMBER11 (Case et al., 2010). cADPR (**1**), cADPcR (**2**) and cADPtR (**3**) were modeled by the General AMBER Force Field (Wang, et al., 2004). AM1-BCC charge (Jakalian, A., Jack, D. B., and Bayly, C. I. (2002). *J. Comput. Chem.* 23, 1623–1641) was used for cADPR and its analogs assigned by Antechamber module (Wang et al., 2006) of AMBER11. In the calculations, interatomic distances restricts were determined by the integrated volumes of the NOESY cross-peaks. As cross peaks of cADPR and cADPcR, previously published data were used (Kudoh, et al., 2005). For generating conformations, we carried out 400 ps simulated annealing molecular dynamics simulations: temperature was decreased from 1000 to 300 K. These simulations were repeated 100 times with different initial velocity for each compound. In calculated conformations, we chose and analyzed the lowest energy conformation.

Acknowledgments: This investigation was supported by a Grant-in-Aid for Grant-in-Aid for Challenging Exploratory Research (2365904901, S. S) from the Japan Society for the Promotion of Science and by Project Grant 084068 from the Wellcome Trust (to Barry V. L. Potter and Andreas H. Guse). Barry V. L. Potter is a Wellcome Trust Senior Investigator (grant 101010).

REFERENCES

Clapper, D. L., Walseth, T. F., Dargie, P. J., and Lee, H. C. (1987). Pyridine nucleotide metabolites stimulate calcium release from sea urchin egg microsomes desensitized to inositol trisphosphate. *J. Biol. Chem.* 262, 9561–9568.

(a) Galione, A. (1993). Cyclic ADP-ribose: A new way to control calcium. *Science* 259, 325–326; (b) Lee, H. C. (1997). Mechanisms of calcium signaling by cyclic ADP-ribose and NAADP. *Physiol. Rev.* 77, 1133–1164; (b) Galione, A., Cui, Y., Empson, R., Iino, S., Wilson, H., and Terrar, D. (1998). Cyclic ADP-ribose and the regulation of calcium-induced calcium release in eggs and cardiac myocytes. *Cell. Biochem. Biophys.* 28, 19–30; (c) Guse, A. H. (1999). Cyclic ADP-ribose: A novel Ca^{2+}-mobilising second messenger. *Cell Signal.* 11, 309–316; (d) Higashida, H., Hashii, M., Yokoyama, S., Hoshi, N., Chen, X. L., Egorova, A., Noda, M., and Zhang, J. S. (2001). Cyclic ADP-ribose as a second messenger revisited from a new aspect of signal transduction from receptors to ADP-ribosyl cyclase. *Pharmacol. Ther.* 90, 283–296; (e) Lee, H. C. (ed.). (2002). *Cyclic ADP-ribose and NAADP: Structures, Metabolism and Functions*. (Kluwer Academic Publishers: Dordrecht); (f) Guse, A. H. (2004). Regulation of calcium signaling by the second messenger cyclic adenosine diphosphoribose (cADPR). *Curr. Mol. Med.* 4, 239–248; (g) Zhang, A. Y. and Li, P. L. (2006). Vascular physiology of a Ca^{2+} mobilizing second messenger—cyclic ADP-ribose. *J. Cell Mol. Med.* 10, 407–422; (h) Jin, D., Liu, H.-X., Hirai, H., Torashima, T., Nagao, T., Lopatina, O., Shnayder, N. A., Yamada, K., Noda, M., Seika, T., Fujita, K., Takasawa, S., Yokoyama, S., Koizumi, K., Shiraishi, Y., Tanaka, S., Hashii, M., Yoshihara, T., Higashida, K., Islam, M. S., Yamada, N., Hayashi, K., Noguchi, N., Kato, I., Okamoto, H., Matsushima, A., Salmina, A., Munesue, T., Shimizu, N., Mochida, S., Asana, M., and Higashida, H. (2007). CD38 is critical for social behaviour by regulating oxytocin secretion. *Nature* 446, 41–45; (i) Venturi, E., Pitt, S., Galfré, E., and Sitsapesan, R. (2012). From eggs to hearts: What is the link between cyclic ADP-ribose and ryanodine receptors? *Cardiovasc. Ther.* 30, 109–116; (j) Lee, H. C. (2012). Cyclic ADP-ribose and nicotinic acid adenine dinucleotide phosphate (NAADP) as messengers for calcium mobilization. *J. Biol. Chem.* 287, 31633–31640.

For examples: (a) Walseth, T. F. and Lee, H. C. (1993). Synthesis and characterization of antagonists of cyclic-ADP-ribose-induced Ca^{2+} release. *Biochem. Biophys. Acta* 1178, 235–242; (b) Lee, H. C., Aarhus, R., and Walseth, T. F. (1993). Calcium mobilization by dual receptors during fertilization of sea urchin eggs. *Science* 261, 352–355; (c) Zhang, F.-J. and Sih, C. J. (1995). Enzymatic cyclization of 1,N6-etheno-nicotinamide adenine dinucleotide. *Bioorg. Med. Chem. Lett.* 5, 1701–1706; (d) Ashamu, G. A., Galione, A., and Potter, B. V. L. (1995). Chemoenzymatic synthesis of analogues of the second messenger candidate cyclic adenosine 5′-diphosphate ribose. *J. Chem. Soc., Chem. Commun*. 1359–1360; (e) Wagner, G. K., Black, S., Guse, A. H., and Potter, B. V. L. (2003). First enzymatic synthesis of an N1-cyclised cADPR (cyclic-ADP ribose) analogue with a hypoxanthine partial structure: Discovery of a membrane permeant cADPR agonist. *Chem. Commun*. 1944–1945; (f) Wagner, G. K., Guse, A. H., and Potter, B. V. L. (2005). Rapid synthetic route toward structurally modified derivatives of cyclic adenosine 5′-diphosphate ribose. *J. Org. Chem.* 70, 4810–4819; (g) Moreau, C., Wagner, G. K., Weber, K., Guse, A. H., and Potter, B. V. L. (2006). Structural determinants for N1/N7 cyclization of nicotinamide hypoxanthine 5′-dinucleotide (NHD+) derivatives by ADP-ribosyl cyclase from aplysia californica: Ca^{2+}-mobilizing activity of 8-substituted cyclic inosine 5′-diphosphoribose analogues in T-lymphocytes. *J. Med. Chem.* 49, 5162–5176; (h) Moreau, C., Kirchberger, T., Zhang, B., Thomas, M. P., Weber, K., Guse, A. H., and Potter, B. V. L. (2012). Aberrant cyclization affords a C-6 modified cyclic adenosine 5′-diphosphoribose analogue with biological activity in Jurkat T cells. *J. Med. Chem*. 55, 1478–1489.

For examples: (a) Galeone, A., Mayol, L., Oliviero, G., Piccialli, G., and Varra, M. (2002). Synthesis of a novel N-1 carbocyclic, N-9 butyl analogue of cyclic ADP ribose (cADPR). *Tetrahedron* 58, 363–368; (b) Huang, L.-J., Zhao, Y.-Y., Yuan, L., Min, J.-M., and Zhang, L.-H. (2002). Syntheses and calcium-mobilizing evaluations of N1-glycosyl-substituted stable mimics of cyclic ADP-ribose. *J. Med. Chem*. 45, 5340–5352; (c) Gu, X., Yang, Z., Zhang, L., Kunerth, S., Fliegert, R., Weber, K., Guse, A. H., and Zhang, L. (2004). Synthesis and biological evaluation of novel membrane-permeant cyclic ADP-ribose mimics: N1-[(5″-O-phosphorylethoxy)methyl]-5′-O-phosphorylinosine 5′,5″-cyclicpyrophosphate (cIDPRE) and 8-substituted derivatives. *J. Med. Chem.* 47, 5674–5682; (d) Xu, J., Yang, Z., Dammermann, W., Zhang, L., Guse, A. H., and Zhang, L.-H. (2006). Synthesis and agonist activity of cyclic ADP-ribose analogues with substitution of the northern ribose by ether or alkane chains. *J. Med. Chem.* 49, 5501–5512; (e) Swarbrick, J. M. and Potter, B. V. L. (2012). Total synthesis of a cyclic adenosine 5′-diphosphate ribose receptor agonist. *J. Org. Chem.* 77, 4191–4197; (f) Yu, P. L., Zhang, Z. H., Hao, B. X., Zhao, Y. J., Zhang, L. H., Lee, H. C., Zhang, L., and Yue, J. (2012). A novel fluorescent cell membrane-permeable caged cyclic ADP-ribose analogue. *J. Biol. Chem.* 287, 24774–24783.

(a) Shuto, S., Shirato, M., Sumita, Y., Ueno, Y., and Matsuda, A. (1998). Nucleosides and nucleotides. 173. Synthesis of cyclic IDP-carbocyclic-ribose, a stable mimic of cyclic ADP-ribose. Significant facilitation of the

intramolecular condensation reaction of N-1-(Carbocyclic-ribosyl)inosine 5′,6″-diphosphate derivatives by an 8-bromo-substitution at the hypoxanthine moiety. *J. Org. Chem.* 63, 1986–1994; (b) Fukuoka, M., Shuto, S., Minakawa, N., Ueno, Y., and Matsuda, A. (2000). An efficient synthesis of cyclic IDP- and cyclic 8-bromo-IDP-carbocyclic-riboses using a modified Hata condensation method to form an intramolecular pyrophosphate linkage as a key step. An entry to a general method for the chemical synthesis of cyclic ADP-ribose analogues. *J. Org. Chem*. 65, 5238–5248; (c) Shuto, S., Fukuoka, M., Manikowsky, M., Ueno, T., Nakano, T., Kuroda, R., Kuroda, H., and Matsuda, A. (2001). Total synthesis of cyclic ADP-carbocyclic-ribose, a stable mimic of Ca^{2+}-mobilizing second messenger cyclic ADP-ribose. *J. Am. Chem. Soc*. 123, 8750–8759; (d) Guse, A. H., Cakir-Kiefer, C., Fukuoka, M., Shuto, S., Weber, K., Matsuda, A., Mayer, G. W., Oppenheimer, N., Schuber, F., and Potter, B. V. L. (2002). Novel hydrolysis-resistant analogues of cyclic ADP-ribose: modification of the "northern" ribose and calcium release activity. *Biochemistry* 41, 6744–6751. (e) Shuto, S., Fukuoka, M., Kudoh, T., Garnham, C., Galione, A., Potter, B. V. L., and Matsuda, A. (2003). Convergent synthesis and unexpected Ca(2+)-mobilizing activity of 8-substituted analogues of cyclic ADP-carbocyclic-ribose, a stable mimic of the Ca(2+)-mobilizing second messenger cyclic ADP-ribose. *J. Med. Chem.* 46, 4741–4749; (f) Kudoh, T., Fukuoka, M., Ichikawa, S., Murayama, T., Ogawa, Y., Hashii, M., Higashida, H., Kunerth, S., Weber, K., Guse, A. H., Potter, B. V. L., Matsuda, A., and Shuto, S. (2005). Synthesis of stable and cell-type selective analogues of cyclic ADP-ribose, a Ca(2+)-mobilizing second messenger. Structure–activity relationship of the N1-ribose moiety. *J. Am. Chem. Soc.* 127, 8846–8855; (g) Hashii, M., Shuto, S., Fukuoka, M., Kudoh, T., Matsuda, A., and Higashida, H. (2005). Amplification of depolarization-induced and ryanodine-sensitive cytosolic Ca^{2+} elevation by synthetic carbocyclic analogs of cyclic ADP-ribose and their antagonistic effects in NG108-15 neuronal cells. *J. Neurochem.* 94, 316–323; (h) Kudoh, T., Murayama, T., Hashii, M., Higashida, H., Sakurai, T., Maechling, C., Spiess, B., Weber, K., Guse, A. H., Potter, B. V. L., Arisawa, M., Masuda, A., and Shuto, S. (2008). Design and synthesis of 4″, 6″-unsaturated cyclic ADP-carbocyclic ribose, a Ca^{2+} mobilizing agent selectively active in T cells. *Tetrahedron* 64, 9754–9765.

(a) Zhang, F.-J., Gu, Q.-M., and Sih, C. J. (1999). Bioorganic chemistry of cyclic ADP-ribose (cADPR). *Bioorg. Med. Chem.* 7, 653–664; (b) Shuto, S. and Matsuda, A. (2004). Chemistry of cyclic ADP-ribose and its analogs. *Curr. Med. Chem.* 11, 827–845; (c) Guse, A. H. (2004). Biochemistry, biology, and pharmacology of cyclic adenosine diphosphoribose (cADPR). *Curr. Med. Chem.* 11, 847–855; (d) Potter, B. V. L. and Walseth, T. F. (2004). Medicinal chemistry and pharmacology of cyclic ADP-ribose. *Curr. Mol. Med.* 4, 303–311.

Lee, H. C. and Aarhus, R. (1993). Wide distribution of an enzyme that catalyzes the hydrolysis of cyclic ADP-ribose. *Biochim. Biophys. Acta* 1164, 68–74.

(a) Lee, H. C., Walseth, T. F., Bratt, G. T., Hayes, R. N., and Clapper, D. L. (1989). Structural determination of a cyclic metabolite of NAD^+ with intracellular Ca^{2+}-mobilizing activity. *J. Biol. Chem.* 264, 1608–1615; (b) Kim, H., Jacobson, E. L., and Jacobson, M. K. (1993). Position of cyclization in cyclic ADP-ribose. *Biochem. Biophys. Res. Commun*. 194, 1143–1147; (c) Lee, H. C., Aarhus, R., and Levitt, D. (1994). The crystal structure of cyclic ADP-ribose. *Nat. Struct. Biol.* 1, 143–144; (d) Gu, Q.-M. and Sih, C. J. (1994). Cyclic ADP-ribose: Synthesis and structural assignment. *J. Am. Chem. Soc*. 116, 7481–7486; (e) Wada, T., Inageda, K., Aritomo, K., Tokita, K., Nishina, H., Takahashi, K., Katada, T., and Sekine, M. (1995). Structural characterization of cyclic ADP-ribose by NMR spectroscopy. *Nucleosides Nucleotides* 14, 1301–1341; (f) Graham, S. M. and Pope, S. C. (2001). NMR solution structure and conformational analysis of the calcium release agent cyclic adenosine 5′-diphosphate ribose (cADPR). *Nucleosides, Nucleotides, Nucleic Acids* 20, 169–183; (g) Graham, S. M., Macaya, D. J., Sengupta, R. N., and Turner, K. B. (2004). cADPR analogues: Effect of an adenosine 2′- or 3′-methoxy group on conformation. *Org. Lett.* 6, 233–236.

Saenger, W. (1983). *Principles of Nucleic Acid Structure*. (Springer, New York, NY).

(a) Reist, E. J., Gueffroy, D. E., and Goodman, L. (1964). Synthesis of 4-Thio-D- and -L-ribofuranose and the corresponding adenine nucleosides. *J. Am. Chem. Soc.* 86, 5658–5663; (b) Bobek, M., Whistler, R. L., and Bloch, A. (1970). Preparation and activity of the 4′-thio derivatives of some 6-substituted purine nucleosides. *J. Med. Chem*. 13, 411–413; (c) Dyson, M. R., Coe, P. L., and Walker, R. T. (1991). The synthesis and antiviral activity of some 4′-thio-2′-deoxy nucleoside analogues. *J. Med. Chem*. 34, 2782–2786; (d) Bellon, L., Barascut, J. L., Maury, G., Divira, G., Goody, R., and Imbach, J. L. (1993). 4′-Thio-oligo-beta-D-ribonucleotides: Synthesis of beta-4′-thio-oligouridylates, nuclease resistance, base pairing properties, and interaction with HIV-1 reverse transcriptase. *Nucleic Acids Res.* 21, 1587–1593. (e) Yoshimura, Y., Watanabe, M., Satoh, H., Ashida, N., Ijichi, K., Sakata, S., Machida, H., and Matsuda, A. (1997). A facile, alternative synthesis of 4′-thioarabinonucleosides and their biological activities. *J. Med. Chem.* 40, 2177–2183; (f) Naka, T., Minakawa, N., Abe, H., Kaga, D., and Matsuda, A. (2000). The stereoselective synthesis of 4′-β-thioribonucleosides via the pummerer reaction. *J. Am. Chem. Soc*. 122, 7233–7243; (g) Takahashi, M., Minakawa, N., and Matsuda, A. (2009). Synthesis and characterization of 2′-modified-4′-thioRNA: A comprehensive comparison of nuclease stability. *Nucleic Acids Res.* 37, 1353–1362.

(a) Elzagheid, M. I., Oivanen, M., Walker, R. T., and Secrist, J. A. III. (1999). Kinetics for the acid-catalyzed hydrolysis of purine and cytosine 2′-Deoxy-4′-thionucleosides. *Nucleosides, Nucleotides, Nucleic Acids* 18, 181–186; (b) Toyohara, J., Gogami, A., Hayashi, A., Yonekura, Y., and Fujibayashi, Y. (2003). Pharmacokinetics and metabolism of 5-125I-iodo-4′-thio-2′-deoxyuridine in rodents. *J. Nucl. Med.* 44, 1671–1676.

Ganellin, C. R. and Owen, D. A. A. (1977). The pressor activity of burimamide: A relationship between chemical constitution and pressor activity of burimamide and related histamine H2-receptor antagonists. *Agents Actions* 7, 93–96.

Hutchinson, E. J., Taylor, B. F., and Blackburn, G. M. (1997). Stereospecific synthesis of 1,9-bis(β-D-glycosyl)adenines: A chemical route to stable analogues of cyclic-ADP ribose (cADPR). *J. Chem. Soc. Chem. Commun.* 1859–1860.

Jeong, L. S., Lee, H. W., Jacobson, K. A., Kim, H. O., Shin, D. H., Lee, J. A., Gao, Z.-G., Lu, C., Duong, H. T., Gunaga, P., Lee, S. K., Jin, D. Z., Chun, M. W., and Moon, H. R. (2006). Structure-activity relationships of 2-chloro-N6-substituted-4′-thioadenosine-5′-uronamides as highly potent and selective agonists at the human A3 adenosine receptor. *J. Med. Chem.* 49, 273–281.

(a) Sekine, M., Nishiyama, S., Kamimura, T., Osaki, Y., and Hata, T. (1985). Chemical synthesis of capped oligoribonucleotides, m7G5′ pppAUG and m7G5′ pppAUGACC. *Bull. Chem. Soc. Jpn*. 58, 850–860; (b) Sekine, M. and Hata, T. (1993). Chemical synthesis of oligonucleotides by use of phenylthio group. *Curr. Org. Chem*. 3, 25–66.

Yoshikawa, M., Kato, T., and Takenishi, T. (1969). Studies of Phosphorylation. III. Selective phosphorylation of unprotected nucleosides. *Bull. Chem. Soc. Jpn*. 42, 3505–3508.

(a) Hancox, E. L. and Walker, R. T. (1996). Some Reactions of 4′-Thionucleosides and Their Sulfones. *Nucleosides Nucleotides* 15, 135–148; (b) Alexandova, L. A., Semizarov, D. G., Krayevsky, A. A., and Walker, R. T. (1996). 4′-Thio-5-ethyl-2′-deoxyuridine 5′-triphosphate (TEDUTP): Synthesis and substrate properties in DNA-synthesizing systems. *Antivir. Chem. Chemther*. 7, 237–242.

Asseline, U. and Thuong, N. T. (1988). Oligothymidylates Substitues Par Un Derive De L'Acridine en Position 5′, A La Fois En Position 5′ et 3′ Ou Sur Un Phosphate Internucleotidique. *Nucleosides Nucleotides* 7, 431–55.

Hata, T., Kamimura, T., Urakami, K., Kohno, K., Sekine, M., Kumagai, I., Shinozaki, K., and Miura, K. (1987). A new method for the synthesis of oligodeoxyribonucleotides bearing a 5′-terminal phosphate group. *Chem. Lett*. 117–120.

Shiwa, M., Murayama, T., and Ogawa, Y. (2002). Molecular cloning and characterization of ryanodine receptor from unfertilized sea urchin eggs. *Am. J. Physiol. Regul. Integr. Comp. Physiol.* 282, R727–737.

(a) Higashida, H., Hashii, M., Fukuda, K., Caulfield, M. P., Numa, S., and Brown, D. A. (1990). Selective coupling of different muscarinic acetylcholine receptors to neuronal calcium currents in DNA-transfected cells. *Proc. Biol. Sci*. 242, 68–74; (b) Amina, S., Hashii, M., Ma, W. J., Yokoyama, S., Lopatina, O., Liu, H. X., Islam, M. S., and Higashida, H. (2010). Intracellular calcium elevation induced by extracellular application of cyclic-ADP-ribose or oxytocin is temperature-sensitive in rodent NG108-15 neuronal cells with or without exogenous expression of human oxytocin receptors. *J. Neuroendocrinol.* 22, 460–466.

(a) Guse, A. H., Roth, E., and Emmrich, F. (1993). Intracellular Ca^{2+} pools in Jurkat T-lymphocytes. *Biochem. J.* 291, 447–451; (b) Guse, A. H., Berg, I., da Silva, C. P., Potter, B. V. L., and Mayr, G. W. (1997). Ca^{2+} entry induced by cyclic ADP-ribose in intact T-lymphocytes. *J. Biol. Chem*. 272, 8546–8550; (c) Schwarzmann, N., Kunerth, S., Weber, K., Mayr, G. W., and Guse, A. H. (2002). Knock-down of the type 3 ryanodine receptor impairs sustained Ca^{2+} signaling via the T cell receptor/CD3 complex. *J. Biol. Chem.* 277, 50636–50642.

Liu, Q., Kriksunov, I. A., Graeff, R., Munshi, C., Lee, H. C., and Hao, Q. (2006). Structural basis for the mechanistic understanding of human CD38-controlled multiple catalysis. *J. Biol. Chem*. 281, 32861–32869.

(a) Juaristi, E. and Cuevas, G. (1992). Recent studies of the anomeric effect. *Tetrahedron* 48, 5019–5087; (b) Thatcher, G. R. J., (ed.), (1993). *The Anomeric Effect and Associated Stereoelectronic Effects*, ACS Symposium Series 539. (Washington DC, American Chemical Society); (c) Juaristi, E. and Cuevas, G. (1995). *The Anomiric Effect*. (CRC Press, Boca Raton); (d) Thibaudeau, C. and Chattopadhyaya, J. (1999). *Stereoelectronic Effects in Nucreosides and Nucreotides and their Structural Implications*. (Uppsala, Uppsala University Press).

Salzner, U. and Schleyer, P. V. R. (1993). Generalized anomeric effects and hyperconjugation in $CH_2(OH)_2$, $CH_2(SH)_2$, $CH_2(SeH)_2$, and $CH_2(TeH)_2$. *J. Am. Chem. Soc.* 115, 10231–10236.

A preliminary account of this study has been published: Tsuzuki, T., Sakaguchi, N., Kudoh, T., Takano, S., Uehara, M., Murayama, T., Sakurai, T., Hashii, M., Higashida, H., Weber, K., Guse, A. H., Kameda, T., Hirokawa, T., Kumaki, Y., Potter, B. V. L., Fukuda, H., Arisawa, M., and Shuto, S. (2013). Design and synthesis of cyclic ADP-4-thioribose as a stable equivalent of cyclic ADP-ribose, a calcium ion-mobilizing second messenger. *Angew. Chem. Int. Ed.* 52, 6633–6637.

Case, D. A., Darden, T. A., Cheatham, T. E. III., Simmerling, C. L., Wang, J., Duke, R. E., Luo, R., Walker, R. C., Zhang, W., Merz, K. M., Roberts, B., Wang, B., Hayik, S., Roitberg, A., Seabra, G., Kolossvary, I., Wong, K. F., Paesani, F., Vanicek, J., Wu, X., Brozell, S. R., Steinbrecher, T., Gohlke, H., Cai, Q., Ye, X., Wang, J., Hsieh, M.-J., Cui, G., Roe, D. R., Mathews, D. H., Seetin, M. G., Sagui, C., Babin, V., Luchko, T., Gusarov, S., Kovalenko, A., and Kollman, P. A. (2010). AMBER 11, University of California, San Francisco.

Wang, J., Wolf, R. M., Caldwell, J. W., Kollman, P. A., and Case, D. A. (2004). Development and testing of a general amber force field. *J. Comput. Chem.* 25, 1157–1174.

Wang, J., Wang, W., Kollman, P. A., and Case, D. A. (2006). Automatic atom type and bond type perception in molecular mechanical calculations. *J. Mol. Graph. Model* 25, 247–260.

Received: 20 December 2014. Accepted: 3 February 2015.